Processing of dynamic visual information in the caudate nucleus

Doctoral Thesis

Péter Gombkötő

2012

Processing of dynamic visual information in the caudate nucleus

Doctoral Thesis

Péter Gombkötő, MSc

Supervisors:

György Benedek, MD, PhD, DSc

Attila Nagy, MS, PhD

Department of Physiology

Faculty of Medicine, University of Szeged

Szeged, 2012

„Intuition tells us that the brain is complicated. We do complicated things, in immense variety. We breathe, cough, sneeze, vomit, mate, swallow, and urinate; we add and subtract, speak, and even argue, write, sing, and compose quartets, poems, novels, and plays; we play musical instruments. We perceive and think. How could the organ responsible for doing all that not be complex?" (David H. Hubel)

List of publications

I. **GOMBKÖTŐ P**, ROKSZIN A, BERENYI A, BRAUNITZER G, UTASSY G, BENEDEK G, NAGY A**,** *Neuronal code of spatial visual information in the caudate nucleus.* **Neuroscience, 182: 225-231, 2011.**

II. ROKSZIN A, **GOMBKÖTŐ P**, BERÉNYI A, MÁRKUS Z, BRAUNITZER G, BENEDEK G, NAGY A, *Visual stimulation synchronizes or desynchronizes the activity of neuron pairs between the caudate nucleus and the posterior thalamus***. Brain Research, 1418: 52-63, 2011.**

III. BERÉNYI A, **GOMBKÖTŐ P**, FARKAS Á, PARÓCZY Z, MÁRKUS Z, AVERKIN R, BENEDEK G, NAGY A. *How moving visual stimuli modulate the activity of the substantia nigra pars reticulata* **Neuroscience, 163: 1316-1326 2009**

Table of content

1 Introduction

One of the several goals of research on the nervous system is to understand how information either from the outside world (i.e.exteroception) or from our internal environment (i.e. interoception) is processed within the system. What computations are necessary? What algorithms are used? How do these transform input into output? What are the resulting behaviors? Last, but not least, where does this processing take place within the system? When we look at the outside world, the primary event is light focusing on an array of 125 million receptors in the retina of each eye. The receptors- rods and cones- are nerve cells specialized to emit electrical signals when light hits them. The task of the rest of the retina and of the brain is to make sense of these signals, to extract biologically relevant information (Hubel, 1995). The above mentioned questions of where and how are applicable to the visual information processing just as well.

Computational theories suggest that any machine carrying out an information processing task may be understood at three levels: first, one should study the goal of its computations; second, the algorithms it uses to perform these computations, and finally the way in which the computations are implemented (Marr, 1982)**.** To our contemporary knowledge, the central nervous system apparatus specialized for visual information processing consists of several levels and functional compartments, the several aspects of the visual input being processed in a parallel manner. However, a considerable number of structures with completely unknown or unclear function remain; therefore, one may draw the conclusion that the picture is far from complete, especially when it comes to complex integration and transfer to the output. Apparently, the complexity of incoming visual information requires such a variety of strategies and structure that it proves to be more efficient to handle them separately. This tendency for attributes such as form, color, and movement to be handled by separate structures in the brain immediately raises the question of how and where all the information is finally assembled. When we say: “the light is bright” or “but that one is brighter” we mean a sensory impression derived from inference, not an exact quantitative comparison. The inference may be quite inaccurate and it may also depend on context variables. Optical illusions illustrate this point well.

Several studies of the relationship between the type of structural defect and the ensuing dysfunction yield valuable hints concerning the whats, hows and whys of normal function. For instance, patients with basal ganglia disorders suffer from excessive or limited movements of the

trunk, arms, or legs. These movement deficits are usually so disabling that deficits of eye movements, if present, may go unnoticed in the course of clinical testing. The basal ganglia are considered to be necessary for the voluntary control of body movements (Delong & Georgopoulos, 1981). To control our movements, we need sensory information about our position against the stationary environment. Hikosaka et al. explored the role of caudate nucleus (CN) in the control of saccadic eye movements. They found several neurons the activity of which, were not associated with the saccadic eye movements and their fire rates were changed by visual and/or auditory stimuli. These visually-responsive neurons had large receptive fields in the contralateral visual field. (Hikosaka, et al., 1989). Previous studies also reported striatal neurons that responded to visual or auditory stimuli (Caan, et al., 1984)

Our hypothesis was that different sensory input transmitted to CN was compared to the copy of motor command transmitted from the area of motor cortex. We assumed that the source of visual information of peripheral visual field was the extrageniculo-extrastriate visual system. This is essential to determine the place of the object which we want to look at or focus our attention on, as fast as possible. The system works without the precise recognition of the object. The geniculo-striate visual system has already recognized what has to be focused upon the fovea centralis. It is well known that motor commands for saccadic eye movements are generated in the frontal eye field (FEF) (Br.8) from lower-level visual input. Precise determination of spatial position of the object is essential for adequate eye positioning. Several experiments confirmed the presence of activity in the CN prior to eye movement, which predicts the saccade (saccade initiation). According to our hypothesis, the copy of motor command is conveyed from the FEF to the system of basal ganglia and it is compared to the predicted sensory signal, which describes the position of the object. It is probable that the required information originates from the extrageniculo-extrastriate visual system. Finally, the copy of the motor command following the explicit recognition contains motor coordinates which has to be transformed into sensory coordinates. This way it can be compared directly to the predicted sensory signal. Another important component of the execution of each motor command is motivation. Dopamine plays an important role in basal ganglia function. (Schultz, 1998). According to Schultz, the dopaminergic neurons of substantia nigra pars compacta (SNc) can determine the importance of the given object by enhancing or suppressing input information to the CN. Movement during fixation of a target results in the relative movement of the peripheral visual field as well. A novel stimulus can appear in the peripheral visual field, but in the described way the subject will only look at it, or observe it if it is significant. A probable

explanation for this is that a facilitation of the predicted signal occurs and the likelihood of the motor command execution increases.

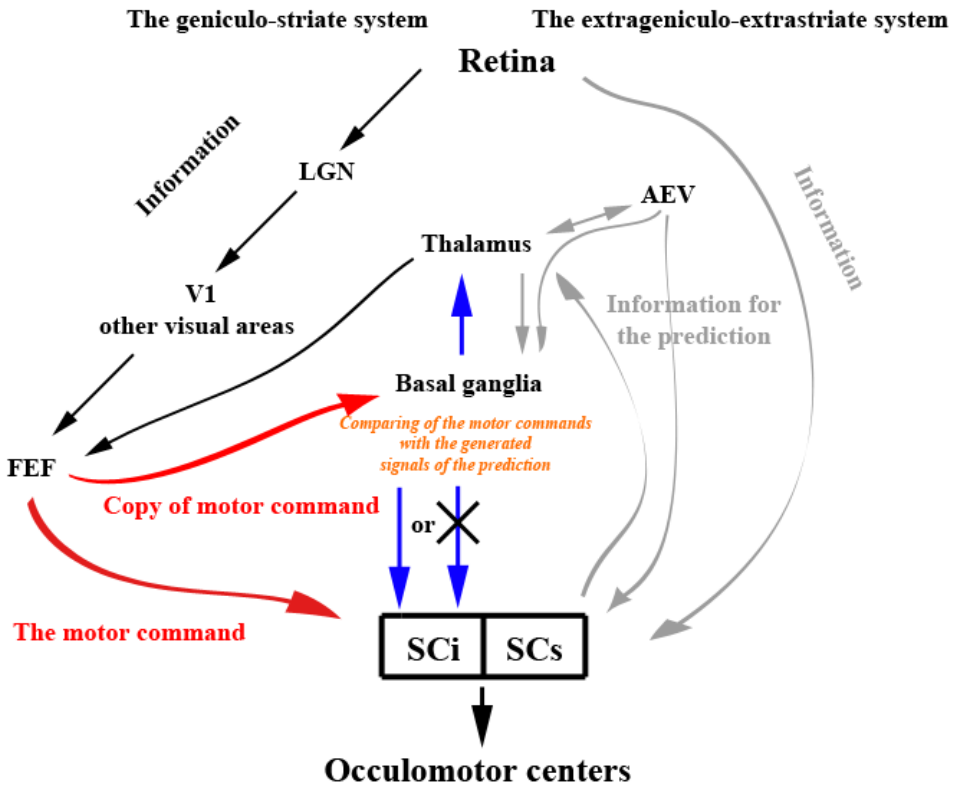

Figure 1. The hypothetic role of the extrageniculo-extrastriate visual information.

Visual information originating from the retina (as shown at the top of the figure) travels in two different ways: through the geniculo-striate system as shown on the left side of the figure and in the extrageniculo-extratrate system, as shown on the right side of the figure. The central structure of the extrageniculo-extrastriato visual system is the superficial layer of the superior colliculus (SCs). The Anterior ectosylvian visual association cortex (AEV) is the cortical part of the system. The frontal eye field (FEF), which is the cortical area responsible for the motor program of voluntary saccades, is shown at the bottom left part of the figure.

The basis of our hypothesis was that the CN, as an input structure of the basal ganglia, receives visual input, which is necessary for the normal function of the basal ganglia. However, there is some degree of uncertainty regarding the pathways conveying sensory information to the basal ganglia. Therefore, we found it an especially interesting question how the extra visual information appears in the CN, how it is interpreted and how it affects the output.

1.1 The caudate nucleus as a station of the tectofugal system.

1.1.1 Anatomical connections between the caudate nucleus and other members of the ascending tectofugal pathway

It was mentioned earlier that there are two major pathways which transmit visual information from the retina to the cerebral cortex in the cat: one of these is the geniculo-striate system, which conveys information to the primary visual cortex via the lateral geniculate nucleus. The other is the extrageniculo-extrastriate system, in which information flows first to the superior colliculus (SC), and then to the suprageniculate nucleus (SG) and lateral posterior pulvinar (PL-Pul) complex of the posterior thalamus, from where a projection leads to what has traditionally been known as association cortices, including the lateral suprasylvian cortex (LS) and the association cortices along the anterior ectosylvian sulcus that include the anterior ectosylvian visual area (AEV), and the insular visual area (IVA) (Benedek, et al., 1988**).** The CN receives input from a large portion of the association cortices and the associated parts of the thalamus, in a more or less topographical manner (Selemon & Goldman-Rakic, 1985; Yeterian & Pandya, 1991). The concept of corticostriatal pathways was earlier widely accepted. Morphological findings in cats and rabbits demonstrated that the corticostriatal pathways send sensory information to the caudate nucleus (Webster, 1965; Norita, et al., 1991; Hollander, et al., 1971). However, an increasing body of evidence is currently accumulating in support of the role of extrageniculate pathways of tectal origin in the sensorimotor integration processes of the basal ganglia (Hoshino, et al., 2009; Nagy, et al., 2003; Nagy, et al., 2008). The dorsolateral aspect of the caudate body in the cat can receive its visual afferentation from the tectum via the suprageniculate nucleus of the thalamus (Harting, et al., 2001; Nagy, et al., 2003; Rokszin, et al., 2011) Recently, a direct projection from the visual association cortex to the caudate nucleus in the feline brain has also been described (Nagy, et al., 2011). The visual inputs of the substantia nigra may originate from the caudate nucleus (Rodríguez, et al., 2000) and from direct (Comoli, et al., 2003) or indirect tectal pathways through the subthalamic nucleus (Kita & Kitai, 1987; Tokuno, et al., 1994; Jiang, et al., 2003) and the pedunculopontine tegmental nucleus (Redgrave, et al., 1987; Lokwan, et al., 1999). The sensory and multisensory receptive field organization of single neurons that we found in these two structures may lend further support to the concept of a tectal, extrageniculate pathway conveying multisensory information to the caudate nucleus and the substantia nigra pars reticulata (Nagy, et al., 2005a; Nagy, et al., 2006).

1.1.2 Properties of neurons in the caudate nucleus

Four major types of neurons were described in the striatum. Medium-sized spiny neurons make up 95% of the total count. They produce γ-aminobutiric acid and constitute the output of the striatum, sending axonal projections to the globus pallidus pars interna (GPi) and substantia nigra pars reticulata (SNr)**.** (Kitka, 1993; Parent, et al., 1984)**.** A smaller portion of CN neurons consists of cholinergic or GABAergic interneurons. Large, aspiny neurons make up 1-2% of the striatal popultion. (Difiglia, et al., 1976; Kawaguchi, et al., 1995) They have extensive axon collaterals in the striatum that terminate on medium spiny neurons. The third main type is the medium aspiny cell. These are also interneurons and are thought to produce somatostatin as transmitter. The fourth type of neuron is a small aspiny cell that stains for parvalbumin. This classification of caudate neurons is based on experiments performed on slice preparations and anesthetized animals (Squire, 2006). In contrast, in awake animals, two types of neurons were identified in the CN: GABAergic projection neurons and cholinergic interneurons (Kawaguchi, et al., 1995). In contrast to the output neurons in the SNr or GPi, which show high spontaneous activity, projection neurons in the striatum are usually very quiet and are difficult to detect by extracellular recording (Hikosaka, et al., 1989; Hikosaka, et al., 2000). They become active only when the animal performs certain tasks. Only a small portion of neurons in the striatum are interneurons. Most prominent among them is a group of neurons that are tonically active. It has been suggested that the tonically active or tonically firing neurons (TFN) are cholinergic interneurons, which correspond to large aspiny neurons and comprise 2% of all striatal neurons (Phelps, et al., 1985; Hikosaka, et al., 2000). The TAN respond to visual or auditory stimuli, but only if the applied stimulus of either modality signifies future reward (Aosaki, et al., 1995).

1.2 The role of the caudate nucleus in visual processing

Sedgwick and Williems (1967) were the first to suggest the existence of visual responsivity in the feline CN (Sedgwick & Williems, 1967; Knudsen, 1982).Several studies in cats and monkeys emphasized the role of the CN in visual information processing (Pouderoux & Freton, 1979; Rolls, et al., 1983; Strecker, 1985; Hikosaka, et al., 1989; Nagy, et al., 2003; Nagy, et al., 2008) It is known that CN neurons are sensitive to various modalities of visual stimulation; both static and dynamic components of visual information are represented here. Thus CN seems to belong to those brain structures, which can sample and evaluate a wide variety of changes in the visual environment. Recent anatomical and physiological studies suggest that CN neurons receive visual

input through the ascending tectofugal system (Hoshino, et al., 2009; Nagy, et al., 2003; Nagy, et al., 2008). The classical visual receptive field properties of the CN neurons (Nagy, et al., 2003) and their sensitivity to visual stimuli of low spatial and high temporal frequency (Nagy, et al., 2008) frequecny (Nagy, et al., 2008) makes them very similar to the neurons in the ascending tectofugal system (Pinter & Harris, 1981; Paróczy, et al., 2006; Márkus, et al., 2009). The visually active neurons in the CN have extremely large visual receptive fields that consistently include the area centralis and cover almost the whole visual field of the contralateral eye (Pouderoux & Freton, 1979; Nagy, et al., 2003). These receptive fields are probably necessary for a proper prediction of the place of the following saccade (Hikosaka, et al., 2000). The overlapping receptive fields should cause a strong redundancy in information transfer if we assume these fields as homogenous. Taking economical and efficacy considerations into account, there should be an alternative information coding algorithm in the CN, which allows a more detailed and thus less redundant processing of visual information. How can CN neurons, within their huge receptive field, determine the location of visual stimuli? Neurophysiological studies demonstrated that single neuronal discharge rate can provide information about the origin of the stimulus within the large receptive field of the neurons for the first time in the optic tectum of birds (Knudsen, 1982). Such panoramic localizers were later described in various species from invertebrates (Bialek, et al., 1991; Nalbach, et al., 1993) to mammals. In the mammalian brain, the structures of the ascending tectofugal system, i.e. the posterior thalamus (Eördegh, et al., 2005) the SC (Jay & Sparks, 1984; Middlebrooks JC, 1984) and also the visual associative cortex along the anterior ectosylvian sulcus (Middlebrooks & Clock, 1994; Middlebrooks, et al., 1998; Middlebrooks, et al., 2002; Benedek, et al., 2004) contain such panoramic localizer neurons. In our studies we investigated if CN neurons are similar to other structures of the ascending tectofugal system in terms of panoramic localizing. As mentioned before, the neurons of CN have large receptive fields, thus, the structure possibly does not localize objects precisely. However, it seems that its visual neurons have a definite preference for different parts of their receptive fields.

2 Aims of the study

The aims of our study were to examine and evaluate the role of the caudate nucleus of the primate and non-primate mammals in visual information processing and to provide further data regarding the coding of dynamic as well as spatial visual information in the striatum. We also intended to provide evidence on the functional connectivity between the CN and the ascending tectofugal system. The concrete aims of our experiments were the following:

1. To investigate the spatial coding abilities of CN neurons and to compare the internal organization of the visual receptive fields in the CN with other structures of the feline brain.
2. To investigate whether the visual CN neurons are panoramic localizers.
3. To investigate whether there is a distributed population code of visual information in the CN so as to acquire a better understanding of the visual representation of the environment in the mammalian brain.
4. To analyze the correlation between the LFPs of the CN and the posterior suprageniculate nucleus of the thalamus (SG) in order to show the synchronized activity of these structures.
5. To verify the existence of visually active neurons in the CN of the primate.
6. To examine the effect of static and dynamic visual stimuli on the activity of the primate CN.

3 Materials and methods

The experimental protocol was accepted and approved by the Ethics Committee for Animal Research of the University of Szeged.

3.1 Animal preparation and surgery - cat

Experiments were performed on 5 adult cats of either sex, weighing between 2.5-4 kg. All experimental procedures were carried out to minimize the number of the animals involved and followed the European Communities Council Directive of 24 November 1986 (86 609 EEC) and the National Institutes of Health guidelines for the care and use of animals for experimental procedures.

The animals were initially anesthetized with ketamine hydrochloride (Calypsol, 30 mg/kg i.m.). To reduce salivation and bronchial secretion, a subcutaneous injection of 0.2 ml 0.1% atropine sulphate was administered preoperatively. After cannulation of the femoral vein and the trachea, animals were placed in a stereotaxic headholder. All wounds and pressure points were treated regularly with local anesthetic (1%, procaine hydrochloride). Throughout the surgery the anesthesia was continued with halothane (Halothane, 1.6%) in air. The animals were immobilized with an initial 2 ml intravenous bolus of gallamine triethiodide (Flaxedil, 20 mg/kg), and artificial ventilation was introduced. During recording sessions, a mixture containing gallamine triethiodide (8 mg/kg/h), glucose (10 mg/kg/h) and dextran (50 mg/kg/h) in Ringer lactate solution was infused continuously at a rate of 4 ml/h. The eye contralateral to the subcortical recording site was treated locally with atropine sulfate (1-2 drops, 0.1%) and phenylephrine hydrochloride (1-2 drops, 10%) to dilate the pupils and block accommodation and to retract the nictitating membranes, respectively, and was equipped with a +2 diopter contact lens. The ipsilateral eye was covered during stimulation and recordings. During the recording session, anesthesia was maintained with a gaseous mixture of air and halothane (1.0%). The depth of anesthesia was monitored by continuously checking the end-tidal halothane concentration and by monitoring heart rate (electrocardiogram) and brain activity (electroencephalogram, EEG). By adjustment of the concentration of halothane, high-amplitude, slow-frequency EEG activity with sleep spindles could be maintained. We also checked repeatedly whether any of the experimental procedures or a forceful pressing of the forepaws might induce resynchronization. The minimum alveolar anesthetic concentration (MAC) values calculated from the end-tidal halothane readings were kept in the range given by Villeneuve and Casanova (Villeneuve & Casanova, 2003). The end-tidal halothane concentration, MAC values and the peak expired CO_2 concentrations were monitored with a capnometer (Capnomac Ultima, Datex-Ohmeda,

ICN). The O_2 saturation of the capillary blood was monitored by pulse oxymetry. The peak expired CO_2 concentration was kept within the range 3.8-4.2% by adjustment of the respiratory rate or volume. The body temperature of the animal was maintained at 37°C by a warm-water heating blanket with an automatic control. Craniotomy was performed with a dental drill to allow a vertical approach to the target structures. The dura mater was preserved, and the skull hole was covered with a 4% solution of 38°C agar dissolved in Ringer's solution.

3.2 Animal preparation and surgery - monkey

Before surgery, the animals were adapted to the laboratory environment and to the primate chair. A scleral search coil was implanted into one eye of monkey, according (Judge, et al., 1980), and at the same time, a stainless steel peg was cemented to the skull for head fixation purposes. The head of monkey was stabilized by the reversible method described in (Pigarev, et al., 1997)**.** A recording chamber was then implanted over the anterior dorsolateral part of the skull (Vogels, 1999a). The position of the recording chamber was determined with the help of magnetic resonance imaging and computerized tomography (CT), both done preoperatively. The centre of the recording chamber was situated 6-7 mm anterior to the interaural plane and 9 mm lateral to the sagittal midline over the left hemisphere in monkey. Recording chambers were implanted over the right hemisphere in each case. Multi electrode driver was implanted into this chamber. Surgical procedures were carried out under full anaesthesia and under aseptic conditions (Kovács, et al., 2003). Anaesthesia was initiated with an i.m. injection of ketamine 8 mg/kg (Calypsol 50mg/ml) and atropine 0.05 mg/kg (atropinum sulfuricum 1 mg/ml). An endotracheal tube was placed into the trachea and throughout the surgery the anesthesia was continued with halothane (Halothane, 1.6%) in air. An i.v. line was inserted for continuous access and additional fentanyl (i.v., 2–4 μg/kg) was administered whenever it was necessary. Before the surgical procedure, a preventive dose of antibiotic was given 500 mg amoxicillin and 100 mg clavulanic acid i.v.; Augmentin 500 mg/100 mg. The same dose was provided i.v. throughout the first five postoperative days. The incision was infiltrated with local anaesthetic (Procaine). Nalbuphin and nonsteroid anti-inflammatory drugs were administered to the animals postoperatively. Arterial oxygen saturation, expired CO_2 level, heart rate, ECG, and rectal temperature were monitored continuously throughout the surgery and kept within physiological range.

3.3 Recording and visual stimulation from anesthetized cat

3.3.1 Recording from the caudate nucleus

Responses of single units were recorded with tungsten microelectrodes (A-M Systems, INC., USA) with an impedance of 2-4 MΩ. Vertical penetrations were made within Horsley-Clarke coordinates for CN neurons sites that were between the coordinates anterior 11-16 and lateral 4-6.5, at stereotaxic depths between 12 and 19 mm. Action potentials were conventionally amplified, displayed on an oscilloscope and transformed through a loudspeaker. The visual responsiveness of the neurons was tested and the extents of the visual receptive fields were estimated subjectively by listening to the responses of the single units to moving visual stimuli generated by a hand-held lamp. Amplified neuronal activity was band-pass filtered between 300 and 3000 Hz. The signal containing multiunit activity was sampled at 20 kHz and stored for off-line analysis (Datawave SciWorks, Version 5.0, DataWave Technologies Corporation, USA). Spikes were extracted after manually adjusted amplitude thresholding, and clustered based on the automatically calculated characteristic parameters of the extracted spike waveforms (peak and trough amplitude and timing, 1st and 2nd principal components). Quality of spike clustering was verified by checking the autocorrelograms of spike trains of the clustered single units (Hazan, et al., 2006)

3.3.2 Stimulation protocol of panoramic localizer neurons

Moving visual noise stimulation (grain size: 0.2-1.5^{o}) was applied for stimulation. The stimuli were moved along four different axes in eight different directions (0 ^{o} -315 ^{o} by 45 ^{o} steps) to find the optimal direction for each unit. This direction was later used to investigate the structure of the visual receptive fields. The stimuli were projected onto a special ellipsoid screen by a projector through a concave lens. The whole visual field of the investigated eye was covered and the projected image was distorted in agreement with the geometric shape of the ellipsoid screen using a combination of a concave Fresnel lens and software based vertex manipulation, so that from the cat's viewpoint the spatial parameters of the stimulus would appear to be uniform along the whole visual field. For the investigation of spatial selectivity, the stimulated area, which practically covered the whole visual field of the investigated eye, was divided into 20 parts or windows of equal size (20^{o} x 15^{o}), and these subunits of the receptive field were stimulated separately. The duration of the pre-stimulus time (stationary whole screen visual noise) was 500 ms, the peri-stimulus time was 2000 ms (the noise pattern in one of the 20 windows was moving in the optimal direction, while the rest of the screen remained stationary) and the post-stimulus time (stationary

whole screen visual noise) was 1000 ms. Each of the 20 parts of the visual field was stimulated with a visual noise 10 times in a random order. The inter-stimulus interval was 1500 ms. Neuronal activity was recorded and correlated with the stimulus presentation offline.

3.3.3 Data analysis of panoramic localizer neurons

The net firing rate, calculated as the difference between the mean firing rates of the cell obtained during peri-stimulus and pre-stimulus time periods was used to characterize the response amplitude of the CN neurons. We defined the firing of a CN neuron during moving visual noise stimulation of a particular part of the visual field as a response, if the Wilcoxon rank-sum test demonstrated significant difference ($p<0.05$) between the pre-stimulus and peri-stimulus firing rate of the cell. The response strength of the neurons was calculated using the following equation:

$$RN_i = \frac{NFR_i}{\max\limits_{1 \le i \le N} NFR_i}$$

where RN_i denotes the responsiveness of a neuron to a stimulus presented at location i; and NFR_i denotes the net firing rate to a stimulus presented at location i.

The spatial selectivity of each responsive CN cell was investigated with one-way analysis of variance (ANOVA). We defined a neuron as spatially selective if the net firing rate of at least one window was significantly different from the mean of the others. Maximum site was defined as the stimulus location at which the net firing rate was the highest. We tested the distribution of sites of maximal sensitivity against uniform distribution using a Pearson chi-square test. Statistical analysis was performed with custom written scripts in the Matlab® software environment (MathWorks ICN., Natick, MA). The visual response onset latencies were calculated using the double sliding windows method developed in our laboratory for a detailed description see (Berényi, et al., 2007)

3.4 Simultaneous recording from the caudate and the suprageniculate nuclei

Vertical penetrations were made within Horsley-Clarke coordinates anterior 4.5 -6-5 and lateral 4-6.5 for SG local field potential (LFP) recordings at stereotaxic depths between 16 and 18 mm, while for CN neurons sites were between the coordinates anterior 12-16 and lateral 4-6.5, at stereotaxic depths between 12 and 19 mm.

Visual event-related LFPs were recorded with tungsten microelectrodes simultaneously from the SG and CN in anesthetized cats. The recorded data, containing the broadband frequency domain, was sampled at 20 kHz, and stored for off-line analysis (Datawave SciWorks, Version 5.0, DataWave Technologies Corporation, USA). The raw signal was digitally filtered between 1-300

Hz. Statistical analysis was performed in the Matlab® software environment (MathWorks ICN., Natick, MA).

3.4.1 LFP Stimulation protocol

For visual stimulation random moving light dots were applied consecutively in each trial. The diameter of each dot was 3 pixels (8.6 min of arc). These random dot kinetograms were generated in the Psychophysics Toolbox extension of Matlab® (Brainard, 1997; Pelli, 1997), and presented on an 18-inch computer monitor (refresh rate: 85 Hz) placed at a distance of 42.9 cm in front of the animal. The steady-state luminance of a stationary dot was 10 cd/m^2, while the background luminance was 2 cd/m^2. The stimulation sequence consisted of 3 phases (Figure 2): first, 1500 ms spontaneous activity was recorded with no stimulation; then, for another 1500 ms, random stationary dots were presented; finally, the same dots were moving for an additional 1500 ms. The stimuli consisted of 200 white dots, and in the dynamic condition these were moving at a speed of 5^o/s. The diameter of each dot was 3 pixels (8.6 mins of arc). This sequence was repeated 500 times.

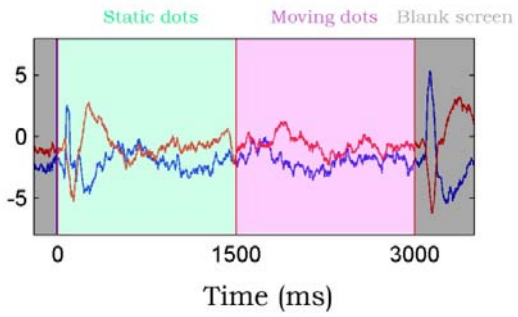

Figure 2. Stimulation paradigm.
Red signal: evoked LFP recorded from SG; blue signal: LFP from CN. Green background: static dot stimulation, pink background: moving dot stimulation; grey background: no stimulation

3.4.2 Data analysis of rhythmicity and synchronization between SG and CN

The current analysis was performed on a pool of 55 recording site pairs. 200 ms-long segments were chosen from six conditions for the analysis and comparison of LFPs. The conditions were: spontaneous activity, onset of static stimulus, continuously static, onset of moving stimulus, moving stimulation, and stimulation offset (Figure 3).

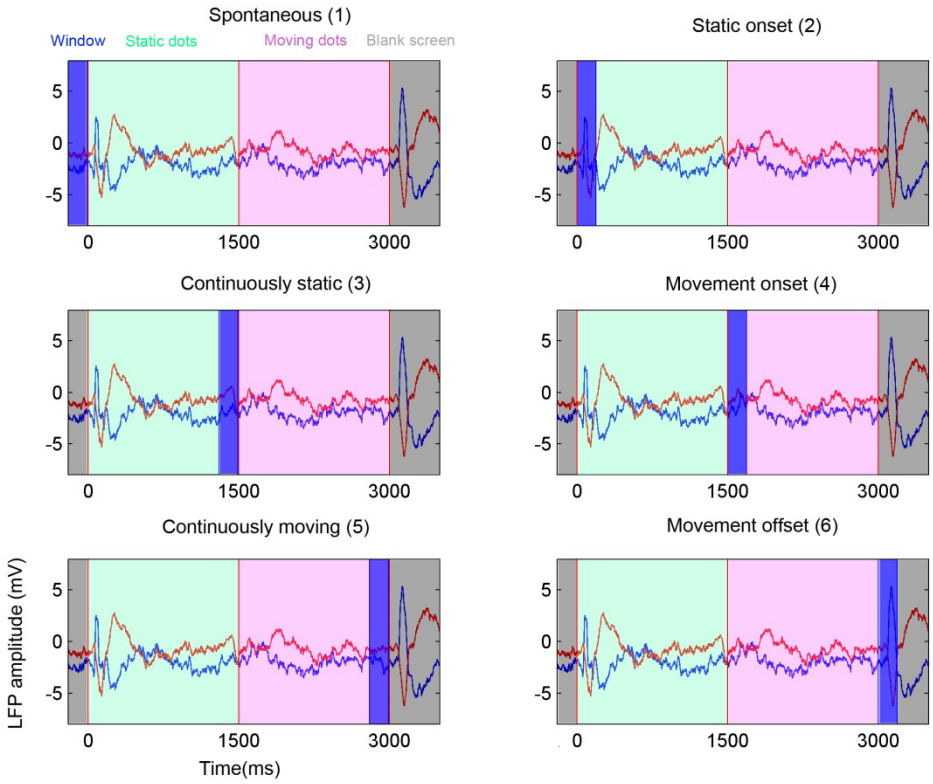

Figure 3. Examined intervals in recorded LFPs

In this figure the sections that were used for the investigation of co-oscillations are highlighted with blue squares. The titles of the subplots and the names of the events (such as Spontaneous, Static onset, etc.) show the name of the section highlighted with the blue square and used for the investigations of synchronization.

Frequency decomposition on each trial was performed. Four different frequency ranges were used. The first range was between 5-8 Hz, in the theta band, the second was between 8-12 Hz, in the alpha band, the third was 12-35 Hz in the beta band, and finally we also examined a broad band between 8-35Hz. To measure the relation between oscillatory spindle co-occurrence at both sites (henceforth: concomitance), we calculated the linear correlation between in the four different range rhythmicity at each site, over windows. Time resolved frequency decomposition of the LFPs was performed by using the Fast Fourier transformation. Concomitance coefficient was used as a measure to reveal the dependence of the contribution of a specific frequency band to the total power of the LFPs' power spectra in the two structures.

$$FFT\%_N = \left(\frac{\int_{f^1}^{f^2} f(PSD)\, d(PSD)}{\int_{f^3}^{f^4} f(PSD)\, d(PSD)} \times 100 \right)_N$$

f_1-f_2:5-8Hz; 8-12Hz; 12-25Hz; 8-35hz; f_3=5 f_4=40Hz, N=number of trials, PSD=Power spectral density

This measure provides an estimate of the tightness of relation in oscillatory content at the two electrodes in a stationary condition, i.e., 'if site one has strong oscillations, does site two also have the same?'. Measurements of rhythmicity between the different orientations were compared with *t*-tests. Across the time windows, we also calculated the cross-correlation coefficient (zero-lag value, which was appropriate for our LFP-LFP relations), providing a measure of the synchronization between the two LFPs (Courtemanche & Lamarre, 2005; Murthy & Fetz, 1996)**.** In contrast to the quantification of similarity in oscillatory profiles, this is a measurement that evaluates the degree of simultaneous change in the recorded signals (Gerstein, 2008; Roelfsema, et al., 1997)**.**

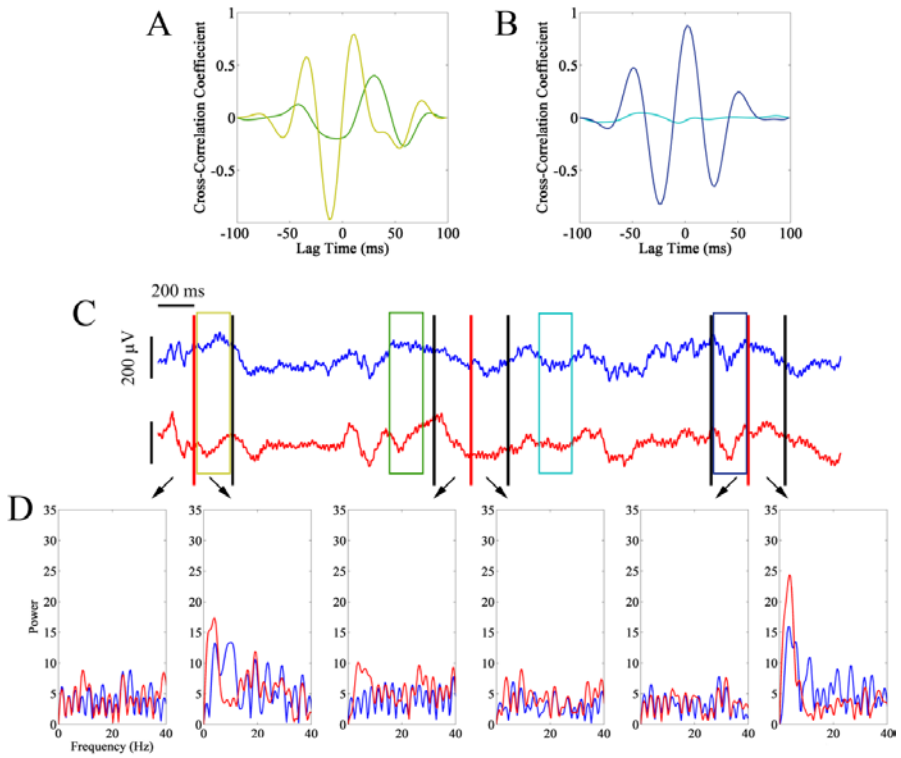

Figure 4. Simultaneous LFP recordings of caudate nucleus and supragenicular nucleus

(A) and (B): snapshots of the temporal evolution of cross-correlation coefficients from the two examined structures.

Different colors signify different points in time, as seen in (C) that shows the two simultaneous trials of LFPs recorded CN (blue) and SG (red), from which (A) and (B) were generated. Cross-correlation (A, B) for each selected period is marked. These periods are highlighted by different colored squares (windows size is 200 ms). (D) The results (PSD) of the Fast Fourier Transforms for each recording site, for each selected period. (200 ms of periods are marked with black and red line).

3.5 Multi- electrode recording from the caudate nucleus of the monkey

Extracellular multielectrode recordings were carried out with 16 implanted platinum-iridium electrodes in the CN of a female monkey (*Macaca mulatta*). For visual stimulation 'center in' and

'center out' optic flow stimuli were applied in a random manner during fixation. The stimuli were generated by the Psychophysics Toolbox of Matlab®. The viewing distance was 57 cm. Positions of dots in sequential frames was changed by two dimensional transformation function. This transformation results in a uniform, homogenous stretch that leaves proportions unchanged and is equal to zooming or magnification. A series of sequential frames was played as a movie. The direction of the transformation (e.g., expansion or contraction) was varied by playing the frame sequence forward or backward. The speed of dots in the flow fields describing the geometry components ranged exponentially from 0^o/sec at the center theoretically, as near the center the dots disappeared) to 7^o/sec at the periphery.

In the applied paradigm the monkey first fixated at a central spot of red light ("Fixation"). During fixation static random dots appeared in the visual field ("Random stationary dots") for 200 ms. After 200 ms the static dots started moving radially as an optic flow for 1000 ms ("Optic flow"). During all phases of the task the monkey had to fixate on a stationary red spot (diameter=1 deg). To exclude the influence of eye movements on neuronal activity the trial was aborted immediately if the animal broke fixation (Figure 5). After successful completion of a trial, the animal received a drop of liquid reward.

During the recording sessions, the monkey was sitting in a primate chair with its head stabilized. A standard 17- inch monitor (at 80 Hz refresh rate) was placed in front of the animal, at a distance of 57 cm. A computer recorded the eye movements (at 250 Hz sampling rate) and delivered the reward. The same computers presented stimuli and collected electrophysiological data by National Instrument DAQ® equipment.

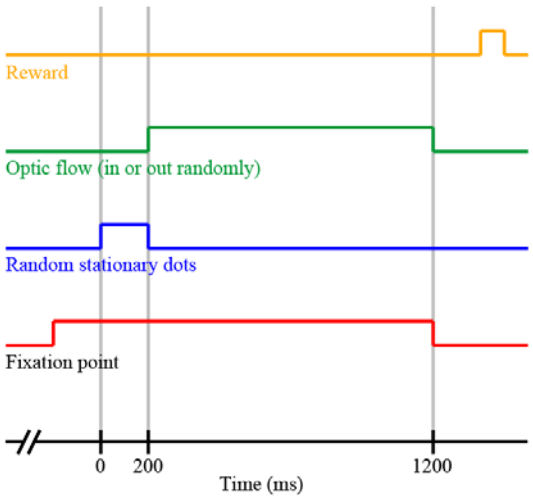

Figure 5. A schematic representation of the stimulation protocol in the monkey experiment.

Red line indicates the presence of the fixation point on the screen. Blue line indicates duration of the presence of static (pre-stimulus time). Green line indicates the optic flow (moving period). Yellow line shows reward.

3.5.1 Data analysis: neurons in the caudate nucleus of the monkey

Unit activity recorded by each electrode was first sorted into single units by the use of KlustaKwik (Harris, et al., 2000) under manual control, and the quality of sorted units was tested by analyzing autocorrelograms and overlays of spike waveforms. According to (Barnes, et al., 2005) we tried to determine the type of neurons on the basis of their auto-correlogram and inter spike (ISI) interval. All statistical analyses were performed using Matlab® (MathWorks Inc., Natick, MA). Spontaneous activity was described with a 1000 ms long intertrial interval from each trials, during which the animal saw a black screen. The recording has been divided up so as to correspond to the phases of the stimulation paradigm. Fixation is constant: that is, in each phase, the animal fixates a central red dot which always precedes the stimulus itself. The first actual stimulation phase was that of static random dots; this was followed by a phase in which these random dots started to move as center-in or center-out optic flow. This latter phase is regarded as the dynamic phase of stimulation. A trial was considered successful if the animal had held fixation throughout. After such trials the animal got reward. Aborted trials - during which the animal had broken fixation - were not followed by reward. Spontaneous activity was defined as intertrial activity. Firing patterns of the static, dynamic and reward phases were compared to spontaneous activity. Differences between successful and aborted trials were also analyzed. We performed statistical analysis in these periods. Statistical comparison was made using the nonparametric Wilcoxon rank-sum test to estimate the significance of the difference ($p<0.05$) between the firing rates.

We used Fast Fourier transform (FFT) to analyze the LFP in 1-50Hz frequency range within the different intervals of stimulation time (pre-stimulus, static stimuli, moving stimuli, post-stimulus time). The whitened power spectral density (PSD) was divided into two frequency ranges, range 1-15 Hz and 20-25 Hz. Ranges were selected subjectively, based on the preliminary data these showed difference in PSD during the stimulation intervals. Percentage of energy content in the selected frequency ranges was calculated to the whole energy content of range 1-50Hz. This calculation was performed according to both of the selected ranges and the four different stimulus times on every trial, and finally we calculated their average:

$$FFTnorm^{\%} = \frac{1}{n} \times \sum_{i=1}^{n} \frac{\int_{f1}^{f2} f(PSD)\, d(PSD)}{\int_{f3}^{f4} f(PSD)\, d(PSD)} \times 100$$

n=number of trials; PSD=Power spectral density; f_1f_2:1-15Hz; 20-25Hz f_3=1 f_4=50Hz

The relative percentages of good trials and aborted trials were compared by two sample t-test, which showed significant difference, that is, the number of good trials significantly differed from that of aborted trials.

4 Results

4.1 Neuronal code of spatial visual information in the caudate nucleus

The visual responses to moving visual noise stimulation of altogether 340 CN neurons were recorded. Eighty-three visually active neurons were found. The internal organization of the visual receptive field of these CN neurons and their spatial coding abilities were analyzed in detail. Most of the recorded units were located between the Horsley-Clarke co-ordinates anterior 11 and 13 and lateral 4 and 6.5, although some visual units were recorded at anterior 14 and 15, too. Histological reconstruction shows the position of visually active CN neurons that were involved in our analysis (Figure 6). These neurons were mostly confined to the caudal portion of the CN and to its dorsolateral part.

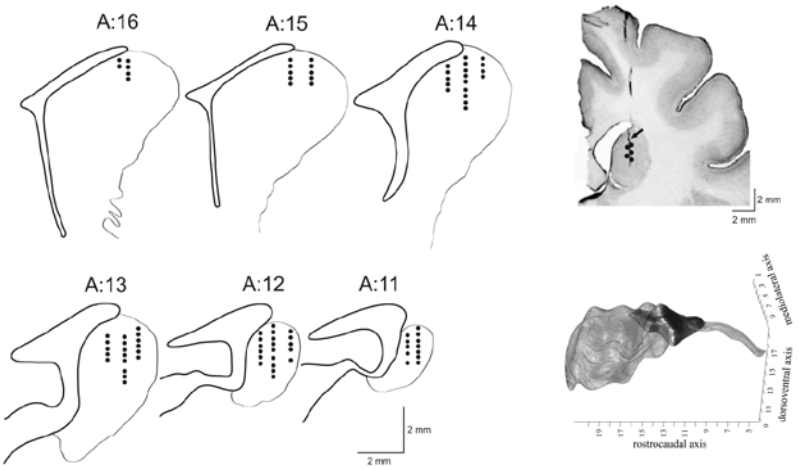

Figure 6. Positions of the analyzed caudate nucleus (CN) neurons.

The drawings depict coronal sections of the CN in the cat brain between A11 and A16 according to the stereotaxic atlas of Snider and Niemer (1964). Filled circles represent the position of the recorded neurons. Scale bars in the bottom right corner provide size calibration and indicate the dorso-ventral and medio-lateral aspects. The insert shows a neutral red-stained section from the CN at about A12 within the electrode track, which is marked by a black arrow. Black dots represent approximate locations of individual neurons.

4.1.1 Extent of visual receptive fields of the caudate nucleus neurons

We analyzed the receptive field properties of the 83 visually active neurons. Similarly to our earlier findings, a subjective estimation of the extents of the visual receptive fields by listening to the neuronal responses to the movements of a light spot generated by a hand-held lamp demonstrated that the visual receptive fields were extremely large, covering a major part of the contralateral hemifield and extending deep into the ipsilateral hemifield, thus yielding a receptive field that overlapped almost totally with the visual field of the contralateral eye (Nagy, et al., 2003; Nagy, et al., 2008) Each visual receptive field covered the area centralis. Together these data rule out the possibility of a retinotopic code of spatial visual information in the CN. An objective

estimation of the extent of the receptive fields also revealed large visual receptive fields in the CN (Figure 7). Similarly to the CN neuron demonstrated (Figure 7), each visually active CN neuron was responsive at a statistically significant level to visual stimulation from a large proportion of the investigated visual field. The median size of the visual receptive fields was 3600 deg^2 (N= 83; range 600-6000 deg^2). Peri-stimulus time histograms (PSTHs) and raster plots were generated during the motion of visual noise.

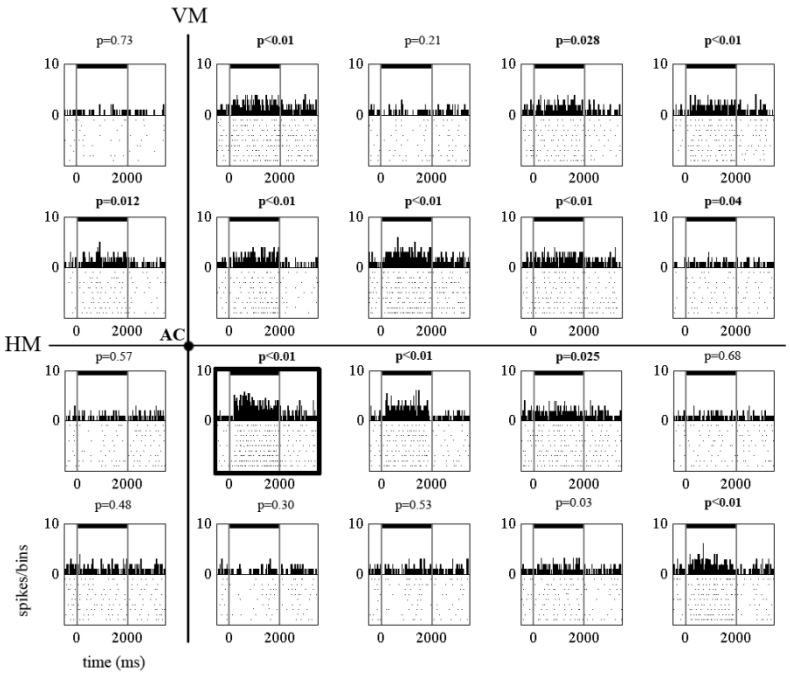

Figure 7. Receptive field organization of a panoramic localizer CN neuron.

Each window represents a 20^o x 15^o portion of the visual field of the investigated eye. In each window, the abscissa indicates time. The ordinate denotes binned action potential numbers (binwidth = 20 ms). The duration of the pre-stimulus time (stationary whole screen visual noise) was 500 ms, the peri-stimulus time (the noise pattern in one of the 20 windows was moving in the optimal direction, while the rest remained stationary) was 1500 ms and the post-stimulus time (stationary whole screen visual noise) was 1000 ms. The three phases of stimulation are separated by vertical lines on each PSTH. The thick black line above each PSTH denotes the duration of the peri-stimulus time. Above each window the p-values of the Wilcoxon rank-sum test are presented. Note the large number of significant responses to visual stimulation from different parts of the receptive field. The thick black box indicates the site of maximum responsiveness within the receptive field. Abbreviations: AC - area centralis, HM - horizontal meridian, VM -vertical meridian.

4.1.2 The visual caudate nucleus neurons serve as panoramic localizers

The most noteworthy finding of the present study is that the visual sensitivity was not homogenous within the huge visual receptive fields of the CN neurons. The analysis revealed that 55 of the 83 visually active CN units (66%) were selective to the location of the visual stimulus, i.e. at least 2 of their responses from different stimulation sites differed significantly from the mean response. (one way ANOVA, $p<0.05$). The huge receptive fields together with the spatial selectivity of the CN neurons suggest that these neurons may serve as panoramic localizers. (Figure 8) shows the responses of a panoramic visual CN neuron that was sensitive to stimulus location. This neuron gave significant responses to the large majority of the stimulus locations tested, with a clear

maximum in the middle of the receptive field (Figure 8). We also investigated the response onset latencies of each CN neuron to visual simulation from different parts of the receptive field and compared these latencies in order to check whether the site of visual stimulation may influence the latency of the CN neurons. The median response onset latency of the CN neurons was 55 ms (range: 15-105 ms). Latency code by the site of stimulation within the receptive field was estimated by means of a one-way analysis of variance. This indicated that none of the investigated CN units showed significantly different latencies depending on the location of the visual stimulus ($p<0.05$).

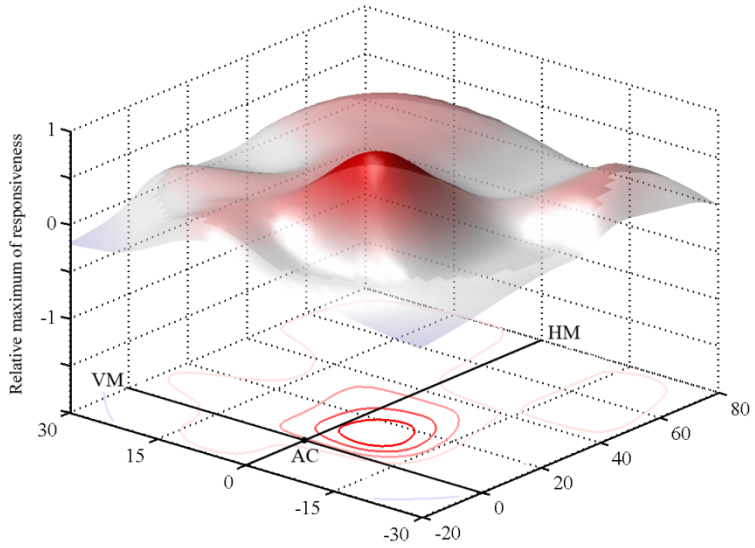

Figure 8. The surface contour plot

The plot shows the visual responsiveness of the same caudate nucleus neuron as in Figure 1. The contours correspond to the relative responsiveness of this neuron to each stimulus site (20^o x 15^o). The area in the lower part of the figure, marked with pink line indicates the sites of the significant responses and thus also denotes the estimated size of the receptive field of this caudate neuron. The thick red ovals show the site of maximum responsiveness of the investigated neuron. For the calculation of relative responsiveness, see methods. Abbreviations: AC - area centralis, HM - horizontal meridian; VM - vertical meridian.

4.1.3 Maximal responsiveness within the large receptive fields

The sites of maximal responsiveness within the large receptive fields varied extensively among the recorded CN cells. (Figure 9) shows the population distribution of the maximal response sites of the 83 visually sensitive panoramic CN neurons. Visual stimulation originating from a particular stimulus site produced a maximal response in some cells, while the rest exhibited preference for other sites. χ^2 test revealed that the distribution of maximum sites was not significantly different from the uniform distribution (χ^2 =2.05; df=19.0; p=0.98), indicating that the maximum sites of the CN neurons were distributed fairly homogenously in the visual field. Thus, each one of the twenty pre-defined windows in the visual field appears to be equally represented within a large population of the panoramic CN neurons.

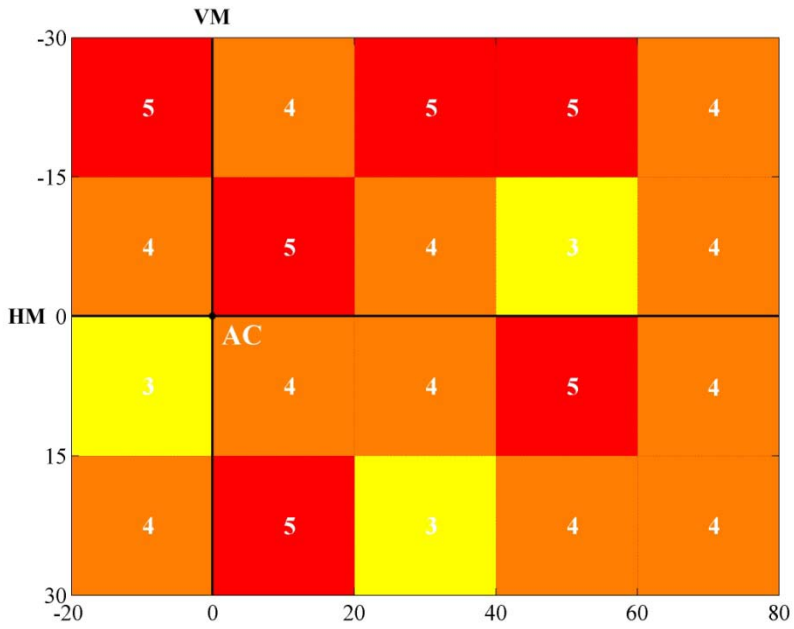

Figure 9. Distribution of sites of maximum sensitivity within the visual field

The sites of maximum responsiveness within the receptive fields of 83 caudate nucleus single-units were determined by searching for the highest firing rate among the stimulation windows. Each square in the figure represents a 20^{o} x 15^{o} size portion of the visual field. The number in each square represents the number of particular neurons that showed maximal responsiveness to stimulation from the given area of receptive field. Note the homogenous distribution of sites of maximum sensitivity. Abbreviations: AC - area centralis, HM - horizontal meridian; VM - vertical meridian.

4.2 Investigation of the physiological connection between the caudate nucleus and the suprageniculate nucleus of the posterior thalamus

4.2.1 Oscillations and synchronization between SG and CN

LFPs were simultaneously recorded from the CN and the SG. In the recorded LFPs the relation between oscillatory spindle co-occurrence at both structures was measured, which we refer to as concomitance. The LFP signals were filtered and divided into four frequency bands. The degree of oscillatory co-occurrence was determined within the examined 200 ms windows (see Methods). Measurements were done in all the four frequency bands. This way we were able to show that changes in the percental energy content of a given band within the LFP recorded from one structure was linked to changes in the percental energy content of the frequency components of the LFP of the other structure. This relation was characterized by a concomitance value. With the help of the six windows it was possible to find out about how concomitance corresponded to the phases of the stimulation paradigm. Figure 10. shows the percentage of relative powers for windows between two simultaneously recorded LFPs in cat.

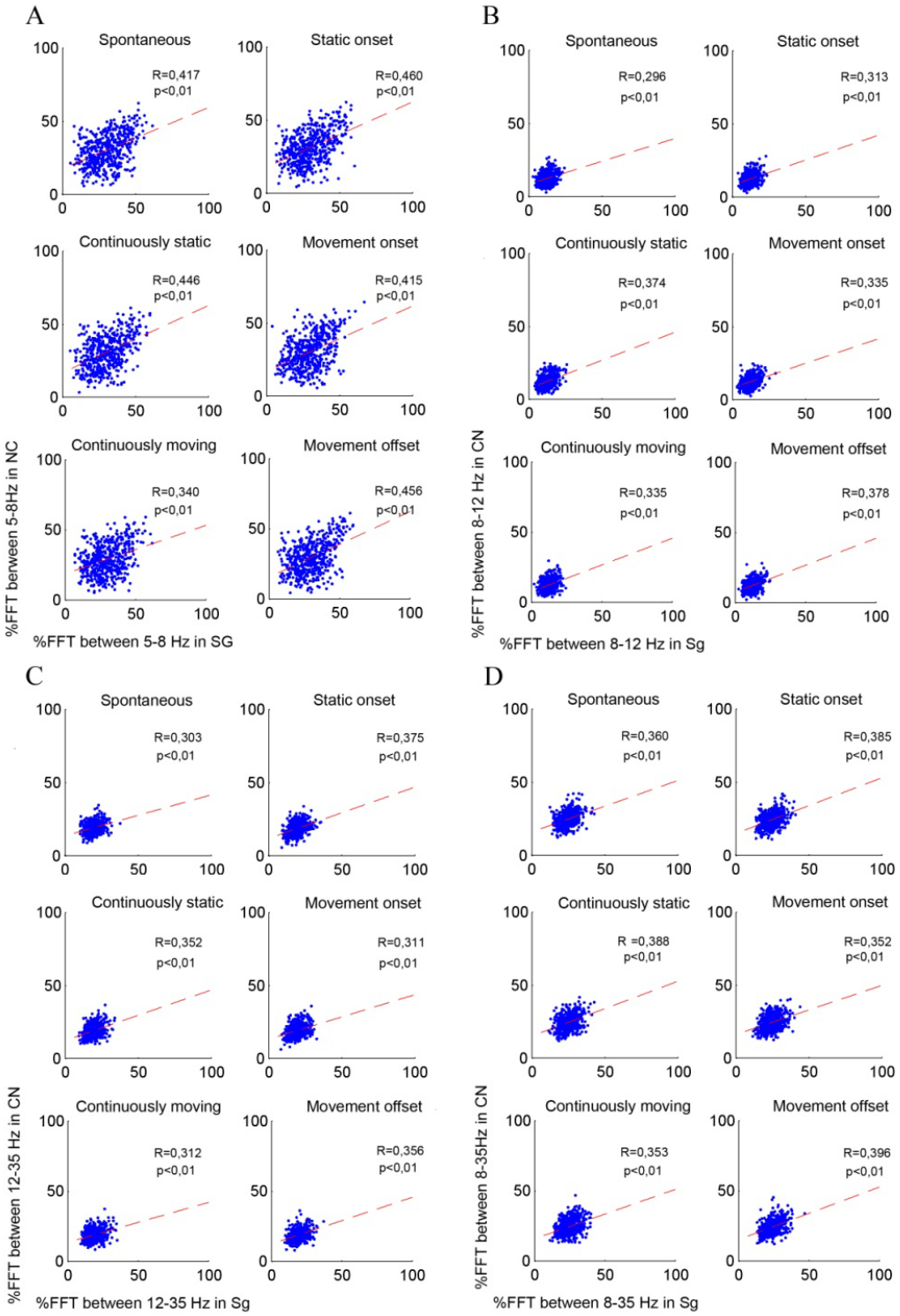

Figure 10. Oscillation properties between SG and CN.

Relationship between the 5-8 Hz (A), 8-12 Hz (C), 12-35 Hz; and (D) 8-35 Hz oscillatory content (FFT% of the LFP signal) at both sites for an SG-CN pair in cat. R: correlation coefficient shows the strength and direction of the linear relationship between two structures. Dashed line: regression line.

The relationship shows a linear correlation expressed as ‘concomitance coefficient’ (Courtemanche & Lamarre, 2005) between different frequency band contents for the LFP pairs (Figure 10). Table 1. contains the R, and p values of linear correlations at different frequency bands.

	5-8 Hz		**8-12Hz**		**12-35Hz**		**8-35Hz**	
	Figure 10 (A)		**Figure 10 (B)**		**Figure 10 (C)**		**Figure 10 (D)**	
	p	*R*	*p*	*R*	*p*	*R*	*p*	*R*
Spontaneous	<0.01	0,417	<0.01	0,296	<0.01	0,303	<0.01	0,360
Static onset	<0.01	0,460	<0.01	0,313	<0.01	0,375	<0.01	0,385
Continuously static	<0.01	0,446	<0.01	0,374	<0.01	0,352	<0.01	0,388
Movement onset	<0.01	0,415	<0.01	0,335	<0.01	0,311	<0.01	0,352
Continuously moving	<0.01	0,340	<0.01	0,335	<0.01	0,312	<0.01	0,353
Movement offset	<0.01	0,456	<0.01	0,378	<0.01	0,356	<0.01	0,396

Table 1. The *R* and the *p* values of concomitance coefficients of CN-SG LFP pairs.

Concomitance coefficients of LFP pairs under different stimulation conditions and in the examined frequency ranges. Values are given as means.

There is a significant correlation of the relative powers of each frequency band in all of the stimulation phases. Table 1. shows the means and standard deviations of concomitance coefficients of CN-SG LFP pairs, shown as divided according to the six stimulation conditions, and four frequency bands. The co-dependence of the relative power of the frequency ranges (concomitance coefficients) are stable during every stimulation segment (Figure 11), which means that the visual stimulation does not decouple the structures of the thalamostriatal pathway in any of the windows or at any of the frequency bands.

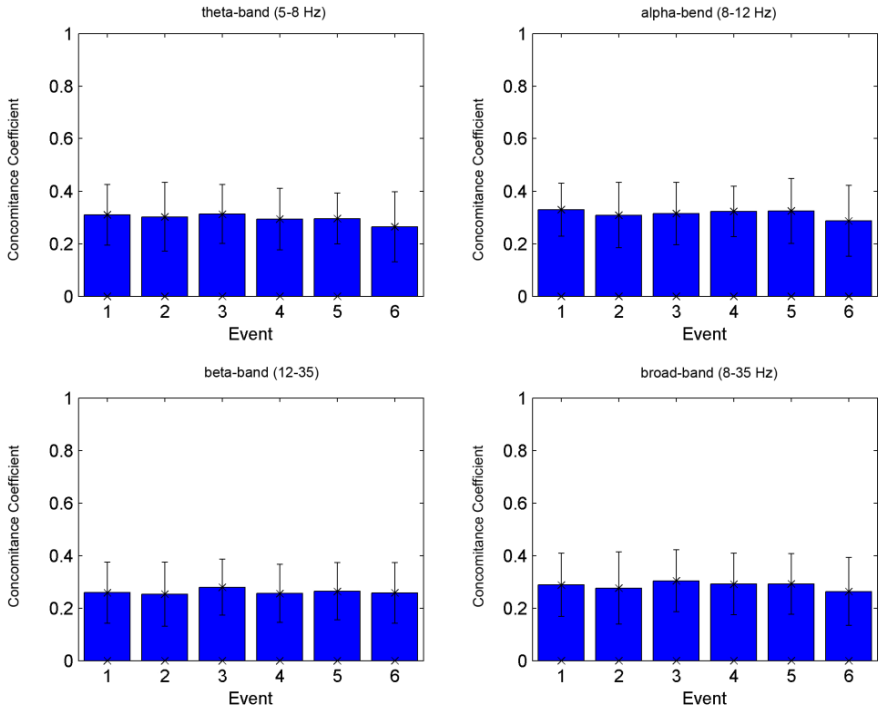

Figure 11. Concomitance coefficients under different stimulation conditions.

Values are given as mean ± SD. The events were: (1) spontaneous activity, (2) onset of static stimulus, (3) continuously static, (4) onset of moving stimulus, (5) moving stimulation, and (6) stimulation offset

After concomitance we investigated the continuous LFPs. We calculated the cross-correlation between the LFPs of SG and CN. We used a moving window of 200ms. This window moved with a 100 ms overlap on the LFPs. LFP cross-correlation coefficients across these windows were measured to evaluate synchronization. We wanted to know if there is any temporal connection of event-related field potentials between the two structures. That is why we used the moving-window cross-correlation. As an example one pair from cat CN is given (Figure 12).

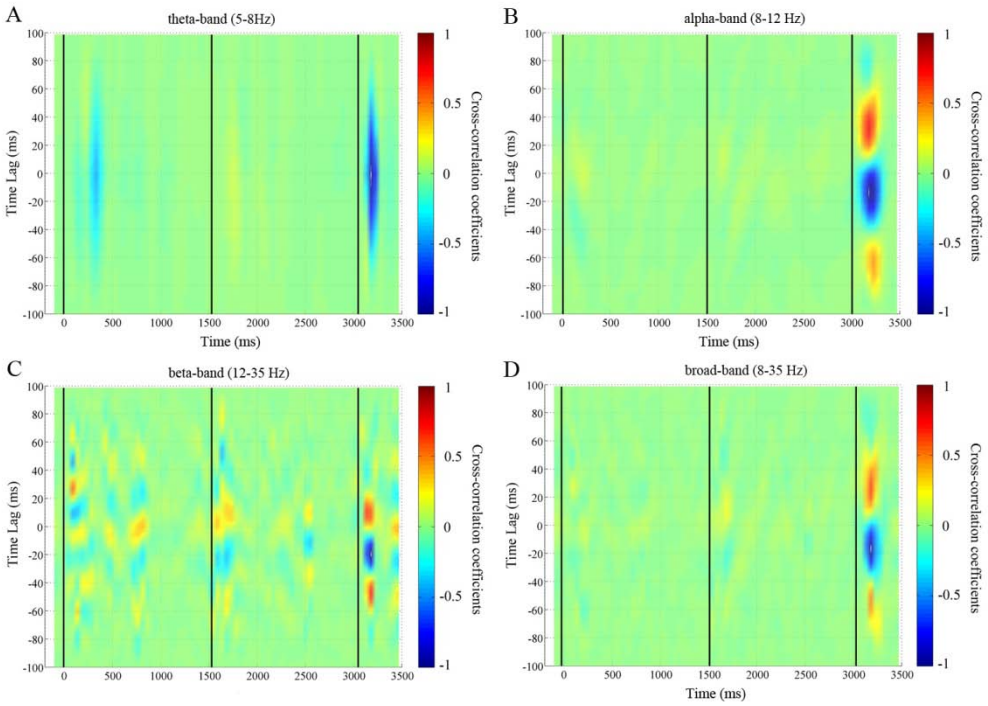

Figure 12. Modulation and synchronization of LFPs in four ranges, for an SG-CN pair.

Color bars show the values of the cross-correlation coefficients. (A) shows the temporal evolution of cross-correlation between LFP pairs in the theta-band (5-8Hz). (B) shows the temporal evolution of cross-correlation between LFP pairs at alpha-band (8-12Hz). (C) shows the temporal evolution of cross-correlation between LFP pairs at beta-band (12-35Hz). (D) shows the temporal evolution of cross-correlation between LFP pairs, broad-band (8-35Hz).

It can be clearly detected that the maximum of the coefficient is at -20 ms at each frequency band. It means that CN is activated after SG. In 56% of cases, SG was activated before CN. Lag time was defined as the temporal position of the maximum value of the correlation coefficient closest to zero in the entire interval. Further maximum values were ignored because the distance between them is equal with the period interval of the given frequency band. The entire temporal evolution was gouged at lag time (Figure 13), so as to show the temporal evolution of the cross-correlation coefficient.

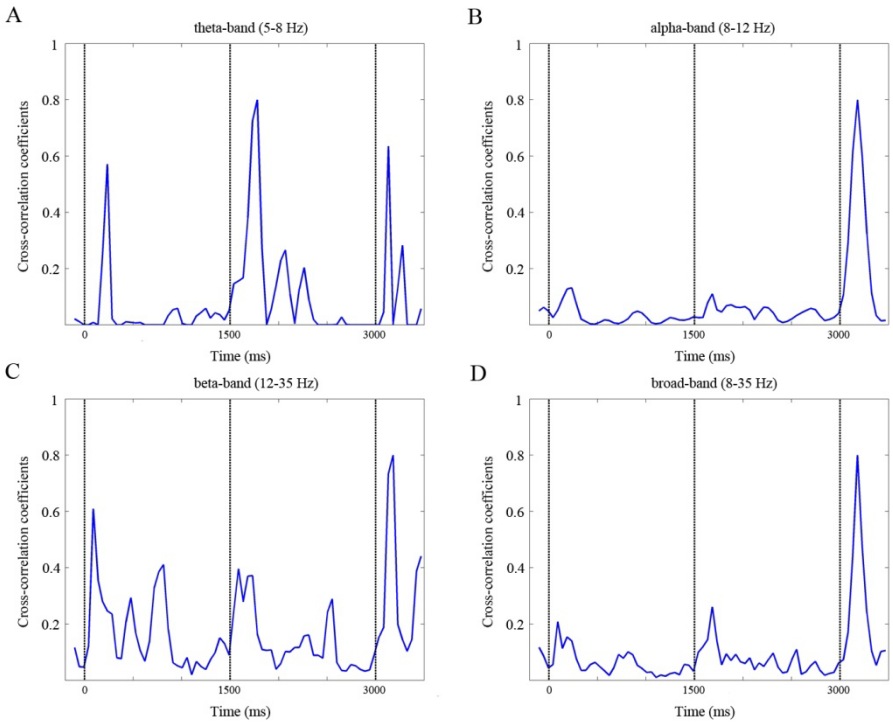

Figure 13. LFP synchronization during the task.

The curves show the cross-correlation coefficient at maximum time lag in the four frequency ranges. For the definition of maximum time lag see text.

It can be seen in Figure 14 that local field potentials recorded from both structures filtered for different frequency bands exhibit correlation in a stimulation paradigm-dependent manner. In the theta-band the flash and disappearance of stimulus resulted in the highest correlation ($0.4<r<0.6$). In the alpha-band the highest cross-correlation coefficient was linked to the disappearance of stimulus ($r=0.8$). In the beta-band the cross-correlation is increased during the stimulation as well, with a mean r of ~0.55).

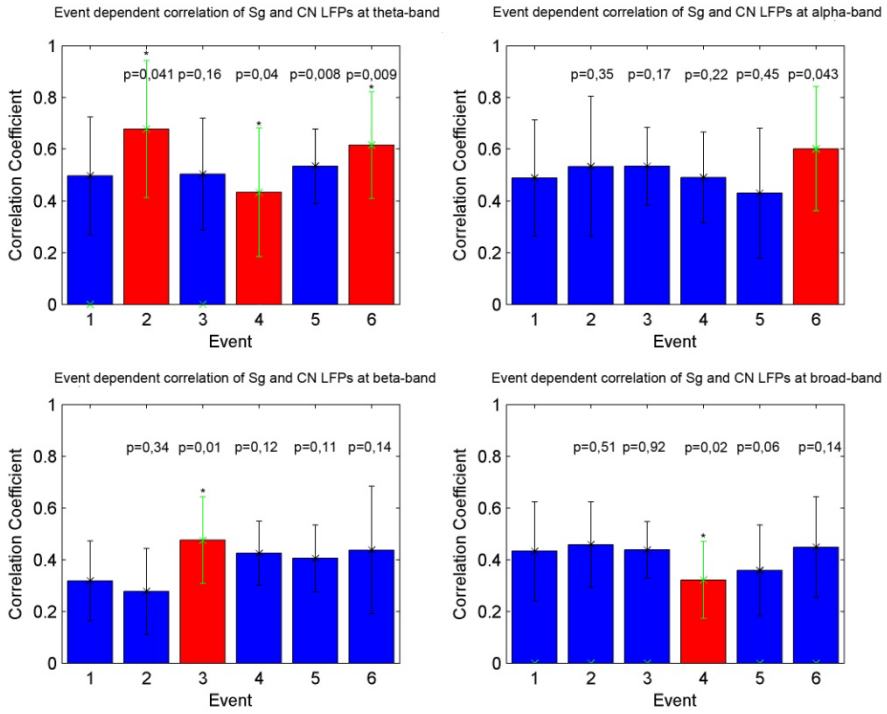

Figure 14. Mean cross-correlation coefficients of LFP pairs in 6 stimulation periods.

Values presented as red bars differ significantly from the cross-correlation coefficient measured during spontaneous activity. The events were: (1) spontaneous activity, (2) onset of static stimulus, (3) continuously static, (4) onset of moving stimulus, (5) moving stimulation, and (6) stimulation offset

We analyzed the cross-correlation coefficients by t-test in six periods of stimulation. We found that tonic stimulation usually increased the correlation of the higher frequency (12-35 Hz) components of the LFP significantly ($p<0.05$), while the phasic events were represented by changes in the lower frequency signal (5-8 Hz) (Figure. 14).

4.3 Optic flow stimulation of CN in monkey

4.3.1 Task-related activity of single units

Task-related responses of putative projection neurons were identified (based on Barnes et al., 2005.) with respect to activity during a 200-msec baseline period of static stimulation (threshold: 2 SDs above baseline mean). Unit data were analyzed per neuron across task events. The histogram of ISI of the projection neurons expands to 2000 ms. The medium-spiny neuron has sharp peak autocorrelogram and the peak in the ISI at two seconds signifies values over 2 seconds. This feature

is characteristic for projection neurons. The amplitude and duration of spikes are higher and longer as compared to interneurons in the CN.

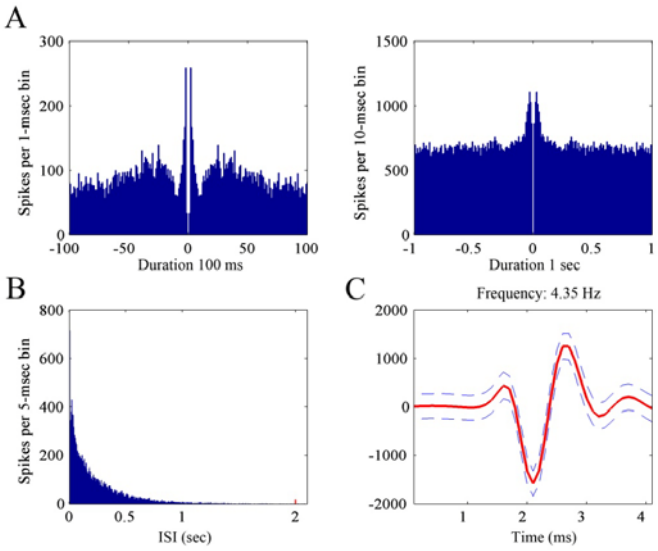

Figure 15. Physiological properties of a putative projection neuron

(A) autocorrelograms (with ± 100 ms and with ±1000 ms windows), (B) ISI plot; The red tick at 2 seconds in (B) signifies the sum of the number of ISIs that have been longer than 2 seconds, and (C) waveform of spike –red line ± 2SD blue line.

The task-related response of projection neuron (n=12) is characterized by increased phasic firing upon visual stimulus onset and at the end of task (Figure 16). During optic flow stimulation the firing rate of the neuron is unchanged. The duration of the phasic activation is 50-100ms. There is a significant difference between the spontaneous activity and the phasic activity. (The basis of our calculations was the distance between the inflection points before and after the maximum of the smooth curve - fitted peri-stimulus time histogram. During optic flow the firing rates do not significantly differ from baseline activity. There is no significant difference between IN and OUT stimulation, neurons do not prefer a certain direction, and there is no significant difference between their firing rates. For OUT stimulation, the mean firing frequency is 3.77 Hz during pre-stimulus time or spontaneous activity, 7.53 Hz during presence of standing dots, 4.26 Hz during presence of moving dots and 8.13 Hz after stimulation, during reward. For IN stimulation, the mean firing frequency is 3.77 Hz during pre-stimulus time, 7.53 Hz during presence of standing dots, 4.26 Hz during presence of moving dots and 8.13 Hz after the stimulation, during reward. In the case of IN-type optic flow the mean firing frequency is 3.84 Hz during pre-stimulus time, 8.18 Hz during presence of standing dots, 3.85 Hz during presence of moving dots and 4.47 Hz after the stimulation during reward. In the case of aborted trials, when the animal does not hold the fixation, the stimulation stops and the task is not rewarded. During this the firing rates do not differ from spontaneous activity, the only significant increase in firing frequency occurs at the beginning of the task.

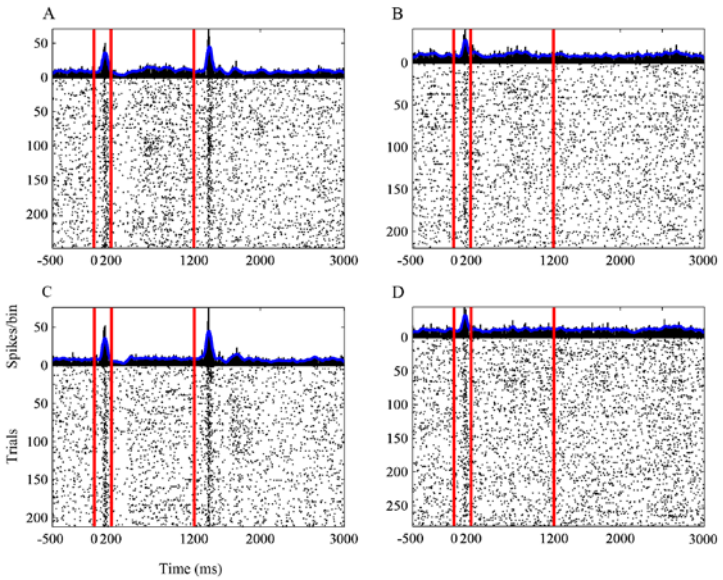

Figure 16. Task-related neuron.

(A) PSTH of OUT stimuli, (B) aborted trials during OUT stimuli, in this case there was no reward (C) PSTH of IN stimuli, (D) aborted trials during IN stimuli, in this case there was no reward.

4.3.2 The activity of reward predictive neurons during stimulation

According to autocorrelation and interspike interval we found putative projection neurons. Responsiveness of these neurons (n=16) is different from the task-related pattern, as described above.

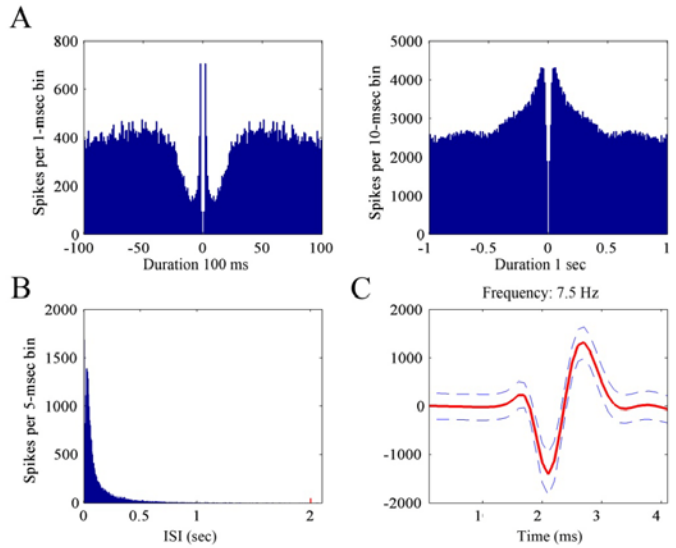

Figure 17. Physiological properties of putative projection neuron.

(A) autocorrelograms (with ± 100 ms and with ±1000 ms windows), (B) ISI plot; The red tick at 2 seconds in B signifies the sum of the number of ISIs that have been longer than 2 seconds., and (C) waveform of spike –red line ± 2SD blue line

The autocorrelation of the neuron starts with a significant peak, it is followed by a steep and finally it becomes constant. The ISI of the neuron is 1500 ms wide. In this case, also the neuron has a sharp peak autocorrelogram and the peak in the ISI at two seconds demonstrates the values over 2 seconds. (Figure 17 B)

The response characteristics of these neurons can be seen in (Figure 18). The firing characteristics of these cells exhibited a decrease upon movement onset, during optic flow the firing frequency started increasing until the physical appearance of reward. Such a gradual firing increase is characteristic of reward prediction, as described in the literature (Schultz, 1998). The purpose of the

following periodic changes in the firing rate is unknown. As for the IN and OUT optic flow, there is no significant difference in the firing rate of the neurons. The firing frequency at rest is 7.14 Hz. During pre-stimulation the firing frequency is 6.9 Hz, and during the statically appearing points it decreases to 5.64 Hz. During optic flow the average frequency is 5.9 Hz, and during the post-stimulus period it reaches even 12.4 Hz.

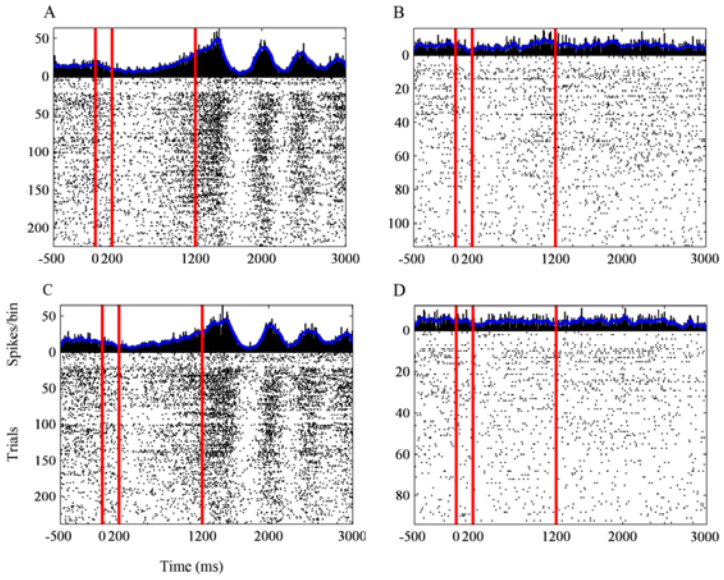

Figure 18. The activity of putative fast spiking neuron.

(A) PSTH of OUT stimuli, (B) An aborted trials during OUT stimuli, in this case there was no reward (C) PSTH of IN stimuli, (D) aborted trials during IN stimuli, in this case there was no reward.

4.3.3 Activity of tonically-firing neurons (TFNs) during optic flow stimulation

Twenty four (n =24) different neuron types were identified. The average firing frequency of the neurons is between 7.25 and 8.60 Hz. There is a wide spilt in their auto-correlogram (Figure 19. A). The ISI is shorter than 1000 ms on average, an interval longer than this is not found between two spikes, see Figure 19 B. According to the electrophysiological parameters, these are cholinergic type neuron.

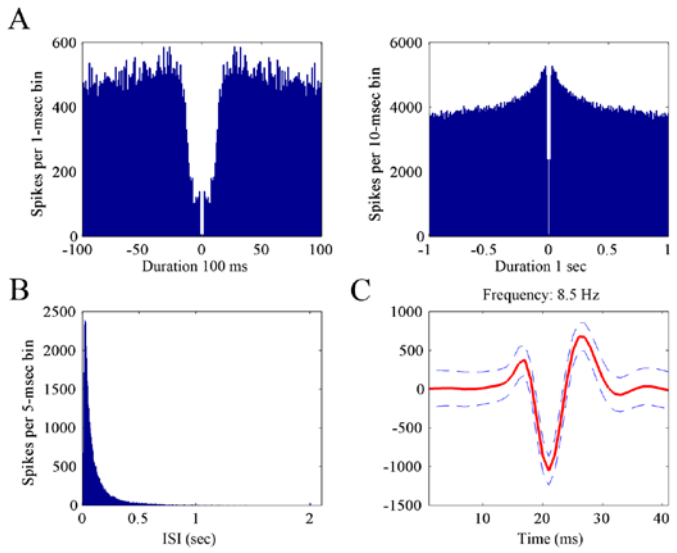

Figure 19. Phsiological properties of putative tonically1-firing neuron.

(A) auto-correlograms (with ± 100 ms and with ±1000 ms windows), (B) ISI plot, and (C) waveform of spike –red line ± 2SD blue line

Visual stimulation results in a higher firing frequency of these cells (Figure 20 A, C). In case of an OUT stimulus, firing frequency was as follows during the different stimulus periods: 9.29 Hz at rest during pre-stimulation period, 8.07 Hz during static point presentation, 12.9 Hz during dynamic stimulation and 8.28 Hz after stimulation, during reward. In case of an IN stimulus: 9.07 Hz during the pre-stimulation period, 9.32 Hz during static point presentation, 13.67 Hz during dynamic stimulation and 7.41 Hz after stimulation. An increase in firing frequency could be seen only in the case of dynamic stimulation. During dynamic stimulation, a significant difference of firing characteristics can be seen, as compared to baseline activity. The direction of optic flow does not lead to a significant difference in firing characteristics (Figure 20 A, C). In the case of aborted trials, no increase in firing frequency could be seen during either moving optic flow or in the post-stimulus interval.

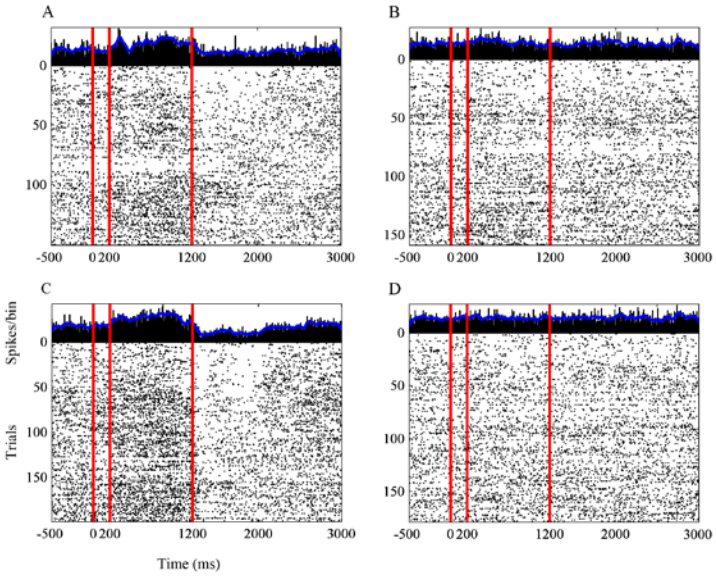

Figure 20. Visual responses of a putative tonically-firing CN neuron

(A) PSTH of OUT stimuli, (B) An aborted trials during OUT stimuli, in this case there was no reward (C) PSTH of IN stimuli, (D) aborted trials during IN stimuli, in this case there was no reward.

4.4 Local filed potentials during task

We investigated the changes caused by 8 different optic flow stimuli paradigms – differentiating IN and OUT types – in two different frequency intervals. In addition, we studied both the successful and aborted trials with regard to the difference in LFP frequency components.

	Names of the investigated epochs
1	Pre-stimulus time with fixation
2	Pre-stimulus time without fixation
3	Static stimuli with fixation
4	Static stimuli without fixation
5	Moving stimuli with fixation
6	Moving stimuli without fixation
7	Pos-tstimulus time with reward
8	Post-stimulus time without reward

Table 2.

A list of the epochs on the basis of which event-related local field potentials were analyzed.

Figure 21 A shows the mean of powers of LFPs during the pre-stimulus interval. (The animal fixated on a red fixation dot on the screen.) In this case optic flow stimulation did not appear, but the colors of curves demonstrate matching values. The appearance of static points does not cause significant change in (Figure 21 B). Upon movement onset, the curves continue to run together in the case of both IN and OUT stimuli. However, in the case of aborted trials, the PSD of bands 1-15 Hz and 20-25 Hz is significantly different, as compared to the ‘normal’ trials (Figure 21 C). Changes during the post-stimulus interval depended on whether the animal received reward or not.

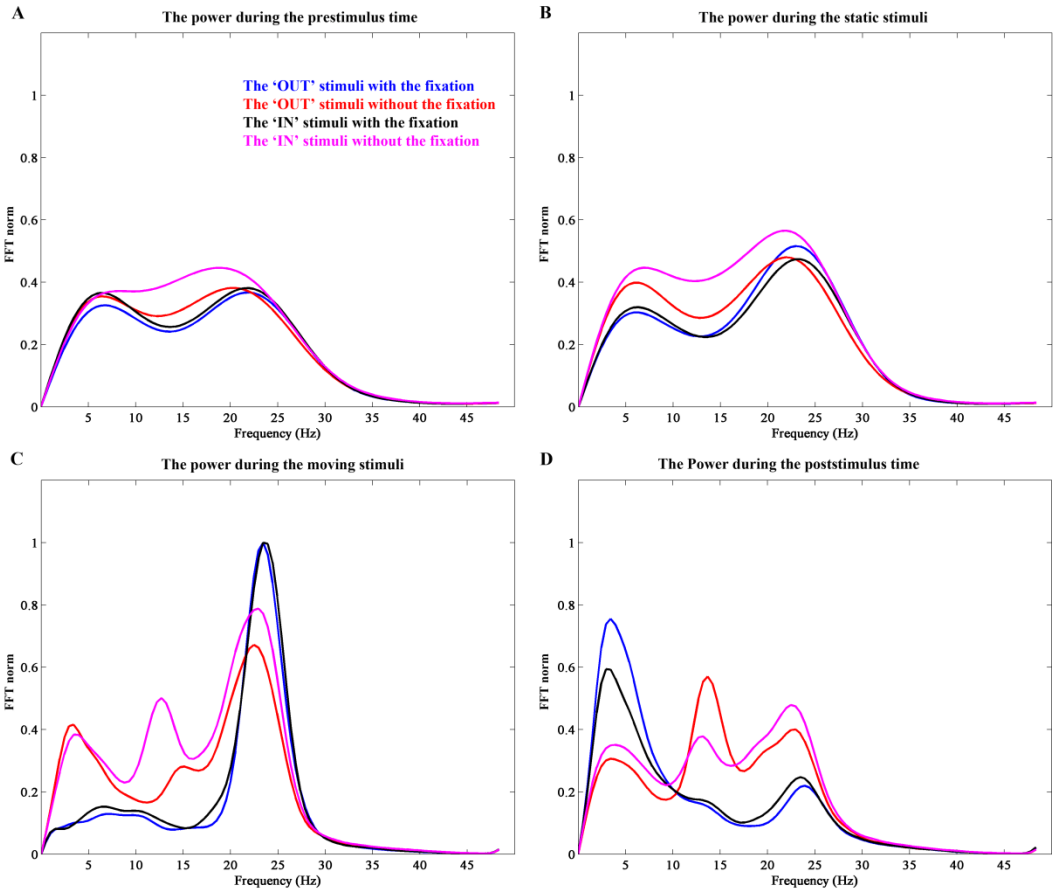

Figure 21. mean of FFT% at different part of LFPs

Each subplot contains four different PSD. The colored curve indicates the type of stimuli and that the stimulation was successful or aborted. (A) shows the power spectral density of LFPs during pre-stimulus time. (B) shows the power spectral density of LFPs during static stimulation. (C) shows the power spectral density of LFPs during dynamic stimulation. (D) shows the power spectral density of LFPs during post-stimlus time.

We analyzed the PSD intervals of 1-15 Hz and 20-25 Hz to determine whether there is any difference between successful and aborted trials.

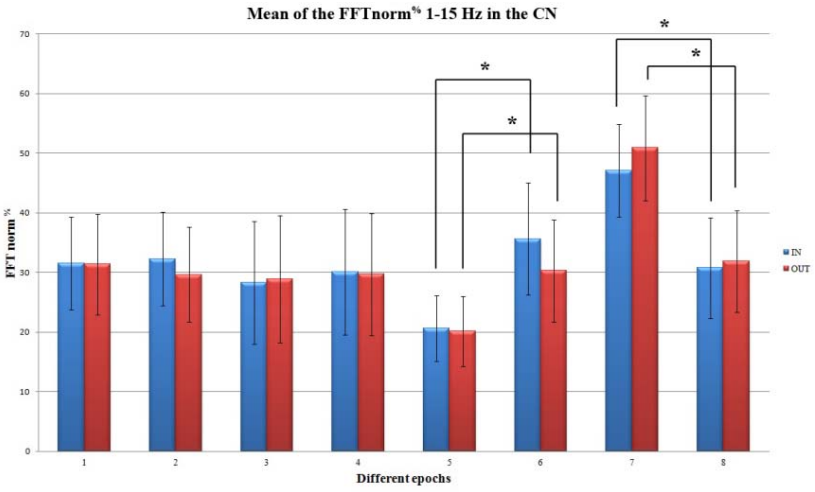

Figure 22. Comparison of the power of frequency range 1-15 Hz in different epochs.

Labels of the X axis correspond to Table1 2. Blue columns refer to trials of IN-type moving stimuli, red columns refer to trials of OUT-type optic flow during dynamic stimulation.

The investigation of the 1-15 Hz band (Figure 22.) revealed that upon the appearance of the moving stimulus the energy power of the frequency intervals in percentage significantly decreases ($p<0.05$) as compared to the energy power of the total spectrum under fixation. If fixation is not complete and the animal cannot perform the task correctly, the decrease significantly differs from the values measured in other epochs. During reward the energy content of this low range was significantly higher than in that case of aborted trials.

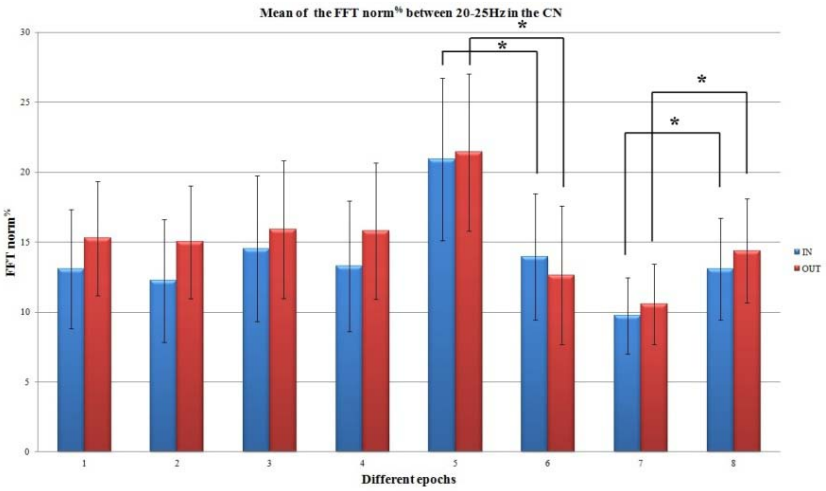

Figure 23. Comparison of the power of frequency range 20-25 Hz in different epochs.

Labels of the X axis correspond to Table1. Blue columns refer to trials of IN-type moving stimuli, red columns refer to trials of OUT-type optic flow during dynamic stimulation.

Analysis of the 20-15 Hz band revealed that optic flow stimulation induces a significant increment in the energy content of the band, in comparison to baseline, provided that the animal fixates. There is also significant difference in this respect between successful and aborted trials ($p<0.05$). If fixation is not complete and the animal cannot perform the task correctly, there is no significant difference from the values measured in other epochs. If fixation is complete, there is significant difference from the values measured in other epochs ($p<0.05$). There is no significant difference between IN and OUT stimulation.

5 Discussion

5.1 Neuronal code of spatial visual information in the caudate nucleus

Our results provide new data concerning the visual representation of the environment in the basal ganglia of the feline brain, suggesting that single neurons in the CN are capable of providing information on the spatial location of visual stimulation.

According to earlier findings, the sensory receptive field of the CN neurons is extremely large (Pouderoux & Freton, 1979; Nagy, et al., 2003). In order to investigate the responsiveness of single CN neurons to visual stimulation arriving from different sites within the receptive field, we divided the huge (practically as large as the visual field of the investigated eye) receptive fields to 20 parts of equal size and stimulated these parts of the receptive field separately. This way we were able to compare the responses of a single CN neuron to stimulation from different stimulus locations. We found that a single visual CN neuron can carry information about stimulus locations throughout the whole physically approachable sensory field. Furthermore, the examined CN neurons exhibited spatial selectivity. It means that any single spatially selective CN neuron could code information on the site of the visual stimulus within its huge receptive field in its firing rate. This way it was possible to read stimulus locations from the firing patterns of single CN neurons. The significant site-selectivity seems to prove that a single CN neuron is able to distinguish between different stimulus locations within its large receptive field. The extremely large receptive fields and the spatial selectivity of the neurons in the CN together suggest that these neurons might serve as panoramic localizers. Although panoramic localizers were described earlier in several cortical and subcortical structures of the mammalian brain (Middlebrooks & Clock, 1994; Middlebrooks, et al., 1998; Benedek, et al., 2004), to our knowledge, we are the first to provide evidence for the same panoramic localization of visual neurons in the CN, the input nucleus of the basal ganglia network.

The huge overlapping receptive fields, which consistently include the area centralis and cover approximately the whole visual field of the investigated eye, do not support the possibility of a classical retinotopic organization in the CN. The absence of such a topographic code in the CN (Pouderoux & Freton, 1979; Nagy, et al., 2003) presupposes an alternative mechanism of spatial visual information coding in this structure. A distributed population code was earlier described for sound source location in the AES cortex (Middlebrooks, et al., 1998; Benedek, et al., 2004) and later for visual stimulus source location in the AES cortex (Benedek, et al., 2004) and the suprageniculate nucleus of the posterior thalamus (Eördegh, et al., 2005) This distributed population code led us to assume that the individual neurons are panoramic localizers. The accurate localization derives from information that is distributed over a large population of such panoramic

neurons. We argue that the accurate coding of the stimulus site might be based on the activity of populations of maximally active CN neurons. The fact that individual visual CN neurons have their sites of maximal sensitivity in different parts of their large receptive field also supports the possibility of a distributed population code in the CN for the localization of visual stimuli. Furthermore, the distribution of sites of maximal sensitivity was uniform within the CN. This means that the peripheral parts of the visual field and the regions around the area centralis are equally represented in the CN, unlike in the geniculostriate system, which exhibits massive overrepresentation of the fovea.

Earlier reports based on the classical visual receptive field and spatio-temporal spectral response properties of the CN suggested that the CN is involved in novelty- and motion detection and less sensitive to static visual stimuli and fine details (Nagy, et al., 2003; Nagy, et al., 2008; Nagy, et al., 2010). The huge receptive fields allow the quick detection of changes in the environment, making the recognition of an event possible per se, without any further details. However, the spatial selectivity of the CN neurons still yields some information about the site of the stimulus (Middlebrooks & Clock, 1994). That the peripheral parts of the visual field and the regions around the area centralis are equally represented in the CN suggests that all of the information reaches the CN with the same probability, independently of the site of stimulation. The panoramic localizing ability of the CN might be useful in rapid behavioral planning, allowing quick detection and response to changes in the environment. This may significantly contribute to and enhance the motor function of the CN, traditionally known as contributing to body and limb posture, and to the accuracy and speed of goal directed movements for a review see: (Villablanca, 2010). Furthermore, during voluntary movement, basal ganglia activity is correlated not only with the motor output, but also with sensory input and perceptual abstractions of these sensory-motor events (Aldridge, et al., 1980), possibly reflecting a connection between motivation and motor output (Nishino, et al., 1991). We argue that the visual activity in the CN may be the sensory feed-back of motor output controlled by the basal ganglia, and therefore it is necessary for the normal sensory-motor function of the CN.

5.2 Synchronization between SG and CN in cat

In order to test the hypothesis that the activity of CN is modulated by the inputs originating in the ascending tectofugal system, we recorded multiscale neuronal activity simultaneously from SG, a thalamic relay nucleus, which transmits the collicular visual information to other structures of the ascending tectofugal system (Norita & Katoh, 1986; Norita, et al., 1991; Katoh, et al., 1995; MacNeil, et al., 1997; Guirado, et al., 2005) and CN (Harting, et al., 2001) of the feline brain. Our

earlier single-cell studies using cross-correlation methods provided the first piece of direct evidence on the functional connection between SG and CN (Rokszin, et al., 2011). These results clearly demonstrated that visual stimulation synchronizes or desynchronizes the activity of CN-posterior thalamus neuron pairs. We analyzed the synchronization between the CN and SG further using local field potentials (LFPs), which allowed us to check for the existence of communication at a population level. Several cortical areas have specific oscillation patterns with well-defined physiological meaning, such as the prefrontal cortex with its 4 Hz oscillation, or the 7-11 Hz hippocampal oscillation (Fujisawa & Buzsáki, 2011)**.** Recently, these oscillations have received more attention from the aspect of synchronization and information transfer. There is a great emphasis on the investigation of the importance of phase locking. We recorded LFPs that transmit extrageniculo-extrastriatal visual information from SG to other ascending tectofugal structures, such as AEV or NC. We analyzed the power of various frequency bands of two structures and we investigated the relationship between the 'co-oscillating' NC and SG populations.

We analyzed the LFP's power of frequency in trials, in 4 ranges compared to the total power of frequency under different stimulation conditions. Concomitance coefficients are stable during every stimulation segment, meaning that the visual stimulation does not decouple the thalamostriatal pathway. Our purpose was to find a relationship between NC and extrastriatal ascending tectofugal visual system and to prove the information transfer between these two structures. The presence of the common frequency components provides evidence of this. NC is in connection with the extrastriato-extrageniculate ascending tectofugal visual system and receives the information that is essential for the coordination of our movements, including the movement of the eyes. Our results provide clear evidence of the synchronization of the two structures' LFPs upon visual stimulation.

The examination of the temporal evolution of cross-correlation revealed when and in what order information transmission between NC and SG occurs and what characteristic frequency bands contain the most information on this crosstalk. In the majority of the cases 56% SG was activated first, while in 36% of the measurements NC activation occurred earlier. This observation suggests a bidirectional flow. However, in the remaining 10%, activation was synchronous, with zero time lag, which might signify common input. The parallel information came from the AEV to the CN and SG, or both of pathways are exist but we proved that there is a functional relationship between SG and CN in processing of visual information. The time lag was between 15 and 20 ms in every case, which might as well be evidence for a direct pathway between these two structures.

5.3 Visual information processing in the CN of monkey

Visual activity in the caudate nucleus has been reported by several laboratories (Pouderoux & Freton, 1979; Rolls, et al., 1983; Strecker, 1985; Hikosaka, et al., 1989; Kolomiets, 1993). In our laboratory we examined the responsiveness of CN neurons in anaesthetized and paralyzed animals and we provided the first description of the visual receptive field properties in the feline CN (Nagy et al., 2003). Visually active neurons were found in the dorsolateral part of the CN caudate nucleus. This region corresponds fully to that reported to receive afferentation from both the extrageniculate visual cortical areas and the extrageniculate visual thalamus (Niida, et al., 1997; Harting, et al., 2001; Guirado, et al., 2005; Nagy, et al., 2011). These CN units prefer intermediate or high velocities, but not low velocities, and most of them exhibit band-pass velocity tuning. Thus, these units are crearly sensitive to the dynamic changes in the visual environment of the animal.

The main goal of this part of the work was to introduce an awake, behaving animal model in our laboratory, allowing us to investigate and analyze the function of the CN in visual information processing. In the monkey experiment, where we used a behavioral fixation paradigm, we tested the effect of the optic flow stimuli (dynamic visual stimulus) on the CN of the primate. This approach- especially when compared to experiments carried out under anaesthesia- yields a fairly realistic electrophysiological picture of the brain and gives us a new chance for the complex investigation of the extrageniculo-extrastriate visual system and the connected basal ganglia. The CN neurons responded optimally to dynamic visual stimulus and were less responsive to stationary visual stimulation. The neurons responded either increased firing rate, while about half of the CN neurons responded with decreased activity during different epochs of the paradigm. The influence of the direction of optical flow (center in or center out) to the responsiveness of each visually active CN neuron was not different. Besides the visually active neurons we also found reward related and task-related CN neurons (Schultz, 1998).

Earlier studies suggested that the CN is involved in visuomotor behavior and contributes to the control of visually guided oculomotor and skeletomotor functions (Lynd-Balta & Haber, 1994; Hikosaka, et al., 2000; Schwarz, et al., 1984; Barneoud, et al., 2000). Based on our results we can conclude that the dynamic component of the visual information is represented in two different ways in the CN. CN neurons either enhance (CN neurons with increased activity) or discontinue (CN neurons with decreased activity) the tonic inhibition of the superior colliculus, and thereby they may help keeping fixation or triggering a saccade.

6 Conclusions

Our results provide new data concerning the visual representation of the environment in the basal ganglia of the feline brain. The lack of retinotopical organization in the CN suggests an alternative non-classic topographical code of spatial visual information here. The single visually active neurons in the CN are capable of providing information via their discharge rate on the spatial location of visual stimulation. The large receptive fields and the spatial selectivity of the neurons in the CN together suggest that these neurons might serve as panoramic localizers. Exact localization is made possible by information that is distributed over a large population of such panoramic neurons. The fact that individual visual CN neurons have their sites of maximal sensitivity in different parts of their large receptive field also supports the possibility of a distributed population code in the CN for the localization of visual stimuli.

In order to test the hypothesis that the activity of CN is modulated by the inputs originating in the ascending tectofugal system, we recorded multiscale neuronal activity simultaneously from SG and CN. Similarly to single-cell studies the synchronization between the CN and SG can also be observed in the low frequency signals (LFPs). These findings show the communication on a population level between SG and CN. The analysis of the power of the investigated frequency bands (4 Hz-35 Hz) in the LFP signals also showed coupling (co-oscillation) between NC and SG neuron populations.

In the monkey experiments, where we taught the animals a behavioral fixation paradigm, we were able to investigate and analyze the role of the CN in optic flow processing. Similar to earlier findings in anaesthetized animals we found that CN neurons responded optimally to dynamic visual stimulus and were less responsive to stationary visual stimulation. The neurons responded with increased firing rate during visual stimulation and can be involved in oculomotor processes. These CN neurons enhance the tonic inhibition of the superior colliculus, and thereby they may help triggering a saccade.

Our findings suggest a strong functional relationship between the ascending tectofugal system and the CN and contradicts significant cooperation between the retinotopically organized geniculo-striate visual system and the CN in the processing of dynamic visual information. We argue that visual activity in the CN may be the sensory feedback of oculomotor and skeletomotor output controlled by the basal ganglia, and therefore it is necessary for the normal sensory-motor function of the CN.

7 Summary

Huge overlapping visual receptive fields and the absence of retinotopic organization in the dorsolateral, caudal part of the caudate nucleus have already been described. In the present study we suggest a possible mechanism for the coding of spatial visual information in this structure. Extracellular microelectrode recordings were carried out in halothane-anesthetized, immobilized, artificially ventilated cats. In order to investigate the responsiveness of the single neurons to visual information arriving from different sites of the receptive field, we divided the visual fields into 20 fields of equal size and stimulated the individual fields one by one. We found that every single visual CN neuron could code information about stimulus locations throughout the whole physically approachable visual field of the investigated eye. The majority (85%) of these neurons exhibited significantly different responses to stimuli appearing in different regions of their huge receptive field. Thus, these neurons appear to have the ability to provide information about the site of the stimulus via their discharge rate. The huge receptive fields in combination with the spatial selectivity suggest that these caudate nucleus neurons may serve as panoramic localizers. At the population level, the sites of maximal responsiveness of the visual neurons are distributed over the whole extent of the receptive fields. We argue that groups of these panoramic localizer neurons with different locations of maximal stimulus preference should have the ability to accurately code the locations of visual stimuli. We propose this distributed population code of visual information as an alternative information processing mechanism.

On the basis of our previous morphological results it was hypothesized that the SG transmits visual information to the CN. Our current hypothesis was that visual stimulation of the extrageniculo-extrastriatal visual system would synchronize the LFP oscillations, indicating synchronous synaptic activity of numerous neurons in CN and SG. Visual event-related LFPs were recorded with tungsten microelectrodes simultaneously from the SG and CN. For visual stimulation random static and moving light dots were used. Time-domain analysis of the responses was performed by calculating the mean linear regression coefficient of the LFP segments. Temporal correlations of the LFPs aquired during each stimulation phase were compared by a t-test for paired samples. Frequency domain decomposition of the LFPs was performed by using the Fast Fourier transformation. Concomitance coefficient was used to characterize the contribution of a specific frequency band to the total power of the LFP power spectra in the two structures. We suggest that there is a strong functional cooperation between the structures, even without visual stimulation. The co-dependence of the relative power of the frequency ranges (concomitance coefficients) are stable during every stimulation segment, meaning that the visual stimulation does not decouple the

thalamostriatal pathway. Tonic stimulation usually increased the cross-correlation of the higher frequency (beta band) components of the LFP, while the phasic stimulation was reflected by changes in the lower (theta) band signal.

The CN, as an input structure of the basal ganglia, is considered to play an important role in the control of oculomotor and skeletomotor processes. In spite of the fact that the motor components of these processes are widely investigated, we have only scarce information about the sensory feedback concerning the motor execution. For completing the motor task, the basal ganglia need sensory information from organisms of the surrounding environment as well. Our aim was that to investigate the effect of optic flow as a dynamically changing visual stimulus on caudate nucleus. A female awake monkey (*Macaca mulatta*) was used in our experiments. Extracellular multielectrode recordings were performed with 16 platinum-iridium electrodes implanted in the CN. During fixation we applied 'center in' and 'center out' optic flow stimulation. The activity of about one third of the investigated CN units (52/165) was modified during task performance. On the basis of the firing pattern we were able to classify neurons into task-related, reward-predictive and tonically firing groups. In addition, we investigated the electrophysiological properties of the neurons according to Barnes, et al., 2005. We assumed the anatomical classification of the neuron (medium-spiny neuron or cholinergic interneuron) based on that study. We found twelve (n=12) task-related neurons based on the firing pattern. According to the electrophysiological properties, these are most probably medium spiny output neurons of the CN. There is no significant difference in the firing pattern with regard to the direction of the optic flow (OUT and IN type of stimuli). The other group of responsive CN neurons is that of reward predictive neurons (n=16) that increase their firing before the reward until the exact moment when the animal is rewarded. Based on the electrophysiological properties of these neurons, these also seem to be medium spiny neurons. Furthermore, we found a third type of neuron in the CN (n=24), which showed significantly increased firing rate during the optic flow compared to the spontaneous activity. An increase in their firing rate is characteristic only of the dynamic stimulation periods, static stimulation did not lead to significant changes as compared to the baseline activity. According to the electrophysiological parameters, these neurons seem to be cholinergic interneurons in the CN. In case of local field potentials two frequency ranges (1-15 Hz and 20-25 Hz) were investigated. Changes in the energy content of field potentials were also analyzed according to their dependence on the type of stimulation. The IN and OUT dynamic visual stimuli did not cause significant changes in the average energy content. Frequency analysis of the LFPs revealed that the percental energy content

of successful dynamic trials and of the reward periods significantly differed from that of aborted trials.

In summary, it has been proven that there are neurons in NC that are capable of coding dynamic visual events in a given part of space. It has also been proven that NC is in a functional relationship with other structures of the tectofugal visual system, such as SG- a possible source of tectal visual information. We have managed to classify neurons in an awake animal based on their general electrophysiological characteristics, and the firing patterns of these neurons upon specific visual stimulation have also been determined. These characteristics allow insight into the complex sensory integration processes of CN, and they may also determine the direction of future research.

8 List of abbreviations

AC - area centralis

AES – anterior ectosylvian sulcus

AEV – anterior ectosylvian visual area

CN – caudate nucleus

FEF – frontal eye field

FFT – Fast Fourier transformation

HM - horizontal meridian

ISI – inter spike intervallum

LFP – Local field potential

LGN – lateral genicuate nucleus

LM-SG – lateral medial suprageniculate nucleus

LS - lateral suprasylvian cortex

PSD – Power spectral density

PSTH – Peristimulus time histogram

SC – superior colliculus

SG – suprageniculate nucleus

TFN – tonically firing neuron

VM – vertical meridian.

9 Acknowledgements

I respectfully thank Professor Dr. György Benedek, Dr. Antal Berényi and Dr. Attila Nagy who have served as my mentors and supervisors, and for the opportunity that I could work with them. I greatly appreciate their helpful and instructive guidance. I express my gratitude to Professor Dr. Gábor Jancsó for allowing me to participate in the Neuroscience Ph.D. Program. My special thanks go to Dr Alice Rokszin, Dr. Zita Márkus, Dr. Gábor Braunitzer for their help and friendship. I would like to acknowledge the help of Györgyi Utassy, Dr. Tamás Nagypál, Anett Nagy, Dr. Wioletta Waleszczyk and Dr. Marek Wypych, too.

I express my most sincere gratitude to Gabriella Dósai for her valuable technical assistance and for the preparation of high-quality figures for my thesis. Many thanks go to Péter Liszli for his expert help in solving hardware and software problems.

I would like to express my thanks to all of my colleagues and friends in the Department of Physiology for their support and kindness. It has been nice to work with them in this department.

My deepest thanks go to Dr. Gabriella Baki and my parents and friends for their continuous love and help in my life and scientific work.

Our experiments were supported by OTKA/Hungary grant T042610, OTKA/Hungary grant 68594.

10 References

Aldridge, J. W., Anderson, R. J. & Murphy, J. T., 1980. Sensory-motor processing in the caudate nucleus and globus pallidus: a single-unit study in behaving primates. *Canadian Journal of Physiology,* Volume 10, pp. 1192-1201.

Aosaki, T., Kimura, M. & Graybiel, A. M., 1995. Temporal and spatial characteristics of tonically active neurons of the primate's striatum. *Journal of Neurophysiology,* Volume 73, pp. 1234-1252.

Barneoud, P., Descombris, E., Aubin, N. & Abrous, D. N., 2000. Evaluation of simple and complex sensorimotor behaviours in rats with a partial lesion of the dopaminergic nigrostriatal system. *European Journal of Neuroscience,* Volume 12, pp. 322-336.

Barnes, T. D. et al., 2005. Activity of striatal neurons reflects dynamic encoding and recoding of procedural memories. *Nature,* Volume 437, pp. 1158-1161.

Benedek, G., Eördegh, G., Chadaide, Z. & Nagy, A., 2004. Distributed population coding of multisensory spatial information in the associative cortex. *European Journal of Neuroscience,* Volume 20, pp. 525-529.

Benedek, G. et al., 1988. Anterior ectosylvian visual area (AEV) of the cat: physiological properties. Volume 75, pp. 245-255.

Berényi, A., Benedek, G. & Nagy, A., 2007. Double sliding-window technique: a new method to calculate the neuronal response onset latency. *Brain Research,* Volume 1178, pp. 141-148.

Bialek, W., Rieke, F., Ruyter van Steveninck, R. & Warlan, R., 1991. Reading a neural code. *Science,* Volume 252, pp. 1854-1857.

Brainard, D. H., 1997. The Psychophysics Toolbox. *Spatial Vision,* Volume 10, pp. 433-436.

Caan, W., Perrett, D. I. & Rools, E. T., 1984. Responses of striatal neurons in the behaving monkey. *Brain Research,* Volume 290, pp. 53-65.

Comoli, E. et al., 2003. A direct projection from superior colliculus to substantia nigra for detecting salient visual events. *Nature Neuroscience,* Volume 6, pp. 974 - 980.

Courtemanche, R. & Lamarre, Y., 2005. Local field potential oscillations in primate cerebellar cortex: synchronization with cerebral cortex during. *Journal of Neurophysiology,* Volume 93, p. 2039–2052.

Delong, M. & Georgopoulos, A., 1981. *Motor function of the basal ganglia.* s.l.:V.B. Brooks.

Difiglia, M., Pasik, P. & Pasik, T., 1976. A Golgi study of neuronal types in the neostriatum of monkeys. *Cerebral Cortex,* Volume 114, pp. 245-256.

Eördegh, G., Nagy, A., Berényi, A. & Benedek, G., 2005. Processing of spatial visual information along the pathway between the suprageniculate nucleus and the anterior ectosylvian cortex. *Brain Research Bulletin,* Volume 67, pp. 281-289.

Fujisawa, S. & Buzsáki, G., 2011. A 4 Hz oscillation adaptively synchronizes prefrontal, VTA, and hippocampal activities. *Neuron,* Volume 72(1), pp. 153-165.

Gerstein, G. L., 2008. Correlation-based analysis methods for neural ensemble data. In: M. A. Nicolelis, ed. *Methods for Neural Ensemble.* Boca Raton (FL): CRC Press, pp. 157-177.

Guirado, S., Real, M. A. & Dávila, J. C., 2005. The ascending tectofugal visual system in amniotes: new insights. *Brain Research Bulletin,* Volume 66, pp. 290-206.

Harris, K. D. et al., 2000. Measurements, ccuracy of tetrode spike separation as determined by simultaneous intracellular and extracellular. *Journal of Neurophysiology,* Volume 84, pp. 401-414.

Harting, K. J., Updyke, V. B. & Van Lieshout, P. D., 2001. Striatal projections from the cat visual thalamus. *European Journal of Neuroscience ,* Volume 14(5), pp. 893-896.

Hazan, L., Zugaro, M. & Buzsáki, G., 2006. Klusters, NeuroScope, NDManager: a Free Software Suite. *Journal of Neuroscience Methods,* Volume 155, pp. 207-216.

Hikosaka, O., Sakamoto, M. & Usui, S., 1989. Functional properties of monkey caudate neurons. II. Visual and auditory responses. *Journal of Neurophysiology,* Volume 61, pp. 799-813.

Hikosaka, O., Takikawa, Y. & Kawagoe, R., 2000. Role of the Basal Ganglia in the Control of Purposive Saccadic Eye Movements. *Physiological Reviews,* Volume 80, pp. 953-978.

Hollander, H., Tietze, J. & Distel, H., 1971. An autoradiographic study of the subcortical projections of the rabbit striate cortex in the adult and during postnatal development. *The Journal of Comparative Neurology,* Volume 184, p. 783–794.

Hoshino, K. et al., 2009. Overlap of nigrothalamic terminals and thalamostriatal neurons in the feline lateralis medialis-suprageniculate nucleus. *Acta Physiologica Hungarica,* Volume 96, pp. 203-211.

Hubel, D. H., 1995. *Eye, Brain, and vision.* 22 ed. s.l.:Scientific American Library.

Jay, M. F. & Sparks, D. L., 1984. Auditory receptive fields in primate superior colliculus shift with changes in eye position. *Nature,* Volume 309, pp. 345-347.

Jiang, H., Stein, B. E. & McHaffie, J. G., 2003. Opposing basal ganglia processes shape midbrain visuomotor activity bilaterally. *Nature,* Volume 424, p. 982–986.

Judge, S. J., Richmond, B. J. & Chu, F. C., 1980. Implantation of magnetic search coils for measurement of eye position: an improved method. *Vision Research,* Volume 20, pp. 535-538.

Katoh, Y. Y., Benedek, G. & Deura, S., 1995. Bilateral projections from the superior colliculus to the suprageniculate nucleus in the cat: a WGA-HRP/double fluorescent tracing study. *Brain Research,* Volume 669, pp. 298-302.

Kawaguchi, Y., Wilson, C. J., Augood, S. J. & Emson, P. C., 1995. Striatal interneurones: chemical, physiological and morphological characterization. *Trends in Neurosciences,* Volume 18, pp. 527-535.

Kita, H. & Kitai, T. S., 1987. Efferent projections of the subthalamic nucleus in the rat: light and electron microscopic analysis with the PHA-L method. *The Journal of Comparative Neurology,* Volume 260, p. 435–452.

Kitka, K., 1993. GABAergic circuits of the striatum. In: G. W. A. a. P. C. Emson, ed. *Chemical Signalling in the Basal Ganglia.* Amsterdam: Elsevier, pp. 51-72.

Knudsen, E. I., 1982. Auditory and visual maps of space in the optic tectum of the owl. *Neuroscience,* Volume 2, pp. 1177-1194.

Kolomiets, B., 1993. A possible visual pathway to the cat caudate nucleus involving the pulvinar. *Experimental Brain Research,* Volume 97, pp. 317-24.

Kovács, G. et al., 2003. Effects of Surface Cues on Macaque Inferior Temporal Cortical Responses. *Cerebral cortex,* Volume 13, pp. 178-188.

Lokwan, S. J., Overton, P. G., Berry, M. S. & Clark, P. G., 1999. Stimulation of the pedunculopontine tegmental nucleus in the rat produces burst firing in A9 dopaminergic neurons. *Neuroscience,* Volume 92, p. 245–254.

Lynd-Balta, E. & Haber, S. N., 1994. Primate striatonigral projections: a comparison of the sensorimotor-related striatum and the ventral striatum. *The Journal of Comparative Neurology,* Volume 345, pp. 562-578.

MacNeil, M. A., Lomber, S. G. & Payne, B. R., 1997. Thalamic and cortical projections to middle suprasylvian cortex of cats: constancy and variation. *Experimental Brain Research,* Volume 114, pp. 24-32.

Márkus, Z. et al., 2009. Spatial and temporal visual properties of the neurons in the intermediate layers of the superior colliculus. *Neuroscience Letters,* Volume 454, pp. 76-80.

Marr, D., 1982. *Vision.* New York: Freeman and Company.

Middlebrooks JC, K. E., 1984. A neural code for auditory space in the cat's superior colliculus. *Journal of Neuroscience,* Volume 4, pp. 2621-2634.

Middlebrooks, J. C. & Clock, A. E., 1994. A panoramic code for sound location by cortical neurons. *Science,* Volume 264, pp. 842-844.

Middlebrooks, J. C., Xu, L., Eddins, A. C. & Green, D. M., 1998. Codes for sound-source location in nontonotopic auditory cortex. *Journal of Neurophysiology,* Volume 80, pp. 863-882.

Middlebrooks, J. C., Xu, L., Furukawa, S. & Macoherson EA, E. A., 2002. Cortical neurones that localize sounds. *Neuroscientist,* Volume 8, pp. 73-83.

Murthy, V. & Fetz, E. E., 1996. Oscillatory activity in sensorimotor cortex of awake monkeys: synchronization of local fi eld potentials and relation to behavior. *Journal of Neurophysiology,* Volume 76, p. 3949–3967.

Nagy, A. et al., 2010. Spectral receptive field properties of visually active neurons in the caudate nucleus. *Neurosci Lett,* Volume 480, pp. 148-153.

Nagy, A., Eördegh, G., Norita, M. & Benedek, G., 2005a. Visual receptive field properties of excitatory neurons in the substantia nigra. *Neuroscience,* Volume 150, pp. 513-518.

Nagy, A., Eördögh, G., Norita, M. & Benedek, G., 2003. Visual receptive field properties of neurons in the caudate nucleus. *Eur J Neurosci,* Volume 18, pp. 449-452.

Nagy, A. J. et al., 2011. Direct projection from the visual associative cortex to the caudate nucleus in the feline brain. *Neuroscience Letters,* 26 September, Volume 503, pp. 52-57.

Nagy, A. et al., 2006. Somatosensory-motor neuronal activity in the superior colliculus of the primate. *Neuron,* Volume 52(3), pp. 525-534.

Nagy, A. et al., 2008. Drifting grating stimulation reveals particular activation properties of visual neurons in the caudate nucleus.. *Eur J Neurosci,* Volume 27, pp. 1801-1808.

Nalbach, H., Thier, P. & Varju, D., 1993. Binocular interaction in the optokinetic system of the crab Carcinus maenas (L.): optokinetic gain modified by bilateral image flow. *Visual Neuroscience,* Volume 10, pp. 873-885.

Niida, T., Stein, B. E. & McHaffie, J. G., 1997. Response properties of corticotectal and corticostriatal neurons in the posterior lateral suprasylvian cortex of the cat. *The Journal of Neuroscience,* Volume 17, pp. 8550-8565.

Nishino, H., Hattori, S., Muramoto, K. & Ono, T., 1991. Basal ganglia neural activity during operant feeding behavior in the monkey: relation to sensory integration and motor execution. *Brain Research Bulletin,* Volume 27, pp. 463-468.

Norita, M. & Katoh, Y., 1986. Cortical and tectal afferent terminals in the suprageniculate nucleus of the cat. *Neuroscience Letters,* Volume 65, pp. 104-108.

Norita, M., McHaffie, G. J., Shimizu, H. & Stein, E. B., 1991. The corticostriatal and corticotectal projections of the feline lateral suprasylvian cortex demonstrated with anterograde biocytin and retrograde fluorescent techniques. *Neuroscience Research,* Volume 10, pp. 149-155.

Parent, A., Bouchard, C. & Smith, Y., 1984. The striatopallidal and striatonigral projections: two distinct fiber systems in primate. *Brain Research,* Volume 303, pp. 385-390.

Paróczy, Z. et al., 2006. Spatial and temporal visual properties of single neurons in the suprageniculate nucleus of the thalamus. *Neuroscience,* Volume 137, pp. 1397-1404.

Pelli, D. G., 1997. The VideoToolbox software for visual psychophysics: Transforming numbers into movies. *Spatial Vision,* Volume 10, pp. 437-442.

Phelps, P. E., Houser, C. R. & Vaughn, J. E., 1985. Immunocytochemical localization of choline acetyltransferase within the rat neostriatum: a correlated light and electron microscopic study of cholinergic neurons and synapses. *The Journal of Comparative Neurology,* Volume 238, pp. 286-307.

Pigarev, N. I., Nothdurft, H. C. & Kastner, S., 1997. A reversible system for chronic recordings in macaque monkeys. *Journal of Neuroscience Methods,* Volume 77, pp. 157-162.

Pinter, R. B. & Harris, L. R., 1981. Temporal and spatial response characteristics of the cat superior colliculus. *Brain Research,* Volume 207, pp. 73-94.

Pouderoux, C. & Freton, E., 1979. Patterns of unit responses to visual stimuli in the cat caudate nucleus under chloralose anesthesia. *Neuroscience Letters,* Volume 11, pp. 53-58.

Redgrave, P., Mitchell, I. J. & Dean, P., 1987. Descending projections from the superior colliculus in rat: a study using orthograde transport of wheatgermagglutinin conjugated horseradish peroxidase. *Brain Research,* Volume 15, pp. 795-803.

Rodríguez, M., Abdala, P. & Obeso, A. J., 2000. Excitatory responses in the 'direct' striatonigral pathway: effect of nigrostriatal lesion. *Movement Disorders,* Volume 15, p. 795–803.

Roelfsema, P. R., Engel, A. K., Kînig, P. & Singer, W., 1997. Visuomotor integration integration is associated with zero time-lag synchronization among cortical areas. *Nature,* Volume 385, p. 157–161.

Rokszin, A. et al., 2011. Visual stimulation synchronizes or desynchronizes the activity of neuron pairs between the caudate nucleus and the posterior thalamus. *Brain research,* Volume 18;1418, pp. 52-63.

Rolls, E. T., Thorpe, S. J. & Maddison, S. P., 1983. Responses of striatal neurons in the behaving monkey. 1. Head of the caudate nucleus. *Behavioural Brain Research,* Volume 7, pp. 179-210.

Schultz, W., 1998. Predictive Reward Signal of Dopamine Neurons. *Journal of Neurophysiology,* Volume 80, pp. 1-27.

Schwarz, M., Sontag, K. H. & Wand, P., 1984. Sensory-motor processing in substantia nigra pars reticulata in conscious cats. *The Journal of Physiology,* Volume 347, pp. 129-147.

Sedgwick, E. M. & Williems, T. D., 1967. Responses of single units in the inferior olive to stimulation of the limb nerves, peripheral skin receptors, cerebellum, caudate nucleus and motor cortex.. *The Journal of Physiology,* Volume 189, pp. 261-279.

Selemon, L. D. & Goldman-Rakic, P. S., 1985. Longitudinal topography and interdigitation of corticostriatalprojections in the rhesus monkey. *The Journal of Neuroscience,* Volume 5, pp. 776-794.

Squire, L. R., 2006. *Fundamental Neuroscience.* Second ed. Philadelphia, PA: Churchill Livingstone.

Strecker, E. R., 1985. Caudate unit activity in freely moving cats: effects of phasic auditory and visual stimuli. *Brain Research,* Volume 329, pp. 350-353.

Tokuno, H., Takada, M., Ikai, Y. & Mizuno, N., 1994. Direct projections from the deep layers of the superior colliculus to the subthalamic nucleus in the rat. *Brain Research,* Volume 639, p. 156–160.

Villablanca, J. R., 2010. Why do we have a caudate nucleus?. *Acta Neurobiologiae Experimentalis,* Volume 70, pp. 95-105.

Villeneuve, M. Y. & Casanova, C., 2003. On the use of isoflurane versus halothane in the study of visual response properties of single cells in the primary visual cortex. *Journal of Neuroscience Methods,* Volume 129, pp. 19-31.

Vogels, R., 1999a. Categorization of complex visual images by rhesus monkeys Part 1: behavioral study. *European Journal of Neuroscience,* Volume 11, pp. 1223-1238.

Webster, E. K., 1965. The cortical-striatal projection in the cat. *Journal of Anatomy,* 99. kötet, pp. 329-37.

Yeterian, E. H. & Pandya, D. N., 1991. Prefrontostriatal connections in relation to cortical architectonic organization in rhesus monkeys.. *The Journal of Comparative Neurology,* Volume 312, pp. 43-67.